Structural Diversity in Thallium Chemistry

Part VI[1])

Analysis of Structure Correlation in Organoammonium Bromothallates(III)

by Anthony Linden*[a]), Alexander Petridis[b]), and Bruce D. James*[b])

[a]) Institute of Organic Chemistry, University of Zürich, Winterthurerstrasse 190, CH-8057 Zürich
[b]) Department of Chemistry, La Trobe University, Vic. 3086, Australia

New bromothallate(III) complexes have been synthesized using eleven organoammonium cations related to others employed previously. The crystal structure determinations of eight of these have been performed. The diethylenetriammonium cation yields the first compound containing $[TlBr_6]^{3-}$ as the only anionic species, while the N,N,N',N'',N''-pentamethyldiethylenetriammonium cation gave a mixed salt containing discrete $[TlBr_4]^-$ and Br^- ions, in which the $[TlBr_4]^-$ unit does not participate in hydrogen bonding. In the pyrazolinium mixed salt, both the $[TlBr_4]^-$ and Br^- ions are hydrogen-bonded to cations and disposed in an arrangement similar to a $[Tl_2Br_9]^{3-}$ unit. The triethylenediammonium dication gives a compound in which a highly distorted trigonal bipyramidal $[TlBr_5]^{2-}$ system is present, while the 1-benzylpiperazinium compound also shows a very weak $[TlBr_4]^-$ and Br^- interaction. Six other monovalent cations provided $[TlBr_4]^-$ derivatives that were characterized either crystallographically or *via* their *Raman* spectra. In a comprehensive structural summary, the various interactions between cations and bromothallate(III) anionic groupings, giving rise to the structural diversity described in this and previous reports, are discussed in terms of the cation charge, quaternization and steric influence, $N-H\cdots Br$ hydrogen bonding, and secondary bonds present in the compounds.

1. Introduction. – Until a few years ago, little was known about the structural diversity displayed by halothallate(III) anions, and, in particular, the bromothallate(III) species. In an extensive study, the use of organic cations has led to the characterization of a range of new bromothallate(III) derivatives. A variety of large univalent cations, encompassing a variety of alkyl diammonium cations [2] and heterocyclic cations [1], have yielded bromothallate(III) complexes of differing stoichiometry. These complexes included, in addition to the well-known $[TlBr_4]^-$ species [3], examples of bromothallate(III) compounds containing unusual mixed salts. For example, the N,N-diethylpropane-1,3-diammonium salt contains each of a $[TlBr_4]^-$ and an axially compressed octahedral $[TlBr_6]^{3-}$ anion, while the hexane-1,5-diammonium complex contains a tetrahedral $[TlBr_4]^-$ anion, a slightly distorted octahedral $[TlBr_6]^{3-}$ and a Br^- anion.

Moreover, further examples of the somewhat lesser known $[TlBr_5]^{2-}$ moieties have also been synthesized. These anions display a range of geometries, such as regular and highly distorted axially-stretched trigonal bipyramidal forms and also *cis*-bromo-

---

[1])   For Part V, see [1].

bridged chains [4–6]. In addition, a bromothallate(III) complex appeared as a distorted octahedron with one long contact from an adjacent anion, thus completing the hexacoordination about an otherwise distorted square pyramid [2], further expanding what was known pertaining to these systems.

In the next phase of this study, reported here, instead of employing an entirely new series of cations, it was decided to focus on the use of a number of other organoammonium cations that are chemically, electronically, or sterically related to those employed in the earlier investigations. This selection of cations allows further comparisons with known bromothallate(III) complexes, and could potentially lead to a clearer picture regarding any controlling relationships between the bromothallate(III) species obtained in the solid state, and the nature of the cation or the synthetic parameters. The eleven cations chosen for this study are depicted in *Table 1*. The introduction of two trivalent cations is to some degree new territory, but these are related structurally to some of the open-chain cations already employed. The crystal structures of eight bromothallate(III) compounds obtained with these cations are described, while the anionic species present in the remaining compounds were deduced from spectroscopic data.

In the second part of this work, as a culmination of our extensive study, the now more substantial library of known structures of organoammonium bromothallate(III) salts is analyzed with the aim of determining if any structure-correlation can be established in terms of the influence of the cation shape, size, charge, quaternization, acidity, or $N-H \cdots Br$ H-bond-donor capabilities on the nature of the anionic species that then appears in the solid state.
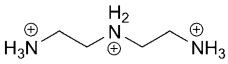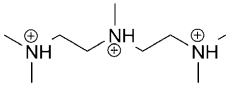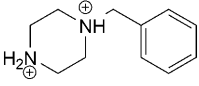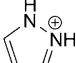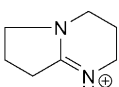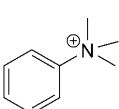
2. Experimental. – 2.1. *Syntheses.* All reagents were obtained from the *Aldrich Chemical Co.*, Milwaukee, WI, and used as received. Solns. of thallium(III) bromide in the chosen solvent were generated from thallium(I) nitrate or sulfate, as described by *Brauer* [7]. *N,N,N′,N″,N″-Pentamethyl*-diethylenetriammonium bromide was synthesized by reacting diethylenetriamine with MeBr, according to the general quaternization procedure of *Oae et al.* [8]. Compounds **1–11**[2])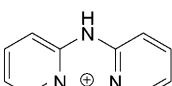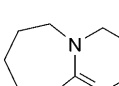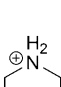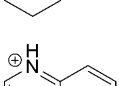 (*Table 2*) were prepared conveniently by mixing the thallium(III) bromide solutions with those containing equimolar quantities of the org. base bromide salts in the same solvent and then warming each mixture to dissolve any resulting precipitate. For crystal growth, various evaporation techniques were employed to minimize the rate of vapor diffusion and solvent loss so that well-formed crystals could be obtained. Generally, several crops of crystals were obtained, and these were isolated by filtration. None of the compounds appeared to be moisture-sensitive, but they were stored routinely in a desiccator over P_2O_5 and KOH.

2.2. Raman *Spectroscopy.* Solid-state *Raman* spectroscopy was employed wherever possible to locate $Tl-Br$ vibrational modes, which are particularly diagnostic for the presence of $[TlBr_4]^-$ species [9]. Spectra were recorded either on a *Dilor XY confocal Raman microprobe* instrument with the 514.3-nm line from a *Spectra Physics 2016* Ar^+ laser, or using a *Renishaw Ramanscope* model *2000* with 633- or 780-nm laser excitation. Even though crystalline samples were crushed, spectra were recorded on crystals of varying orientation and using different polarizations to ensure that any *Raman* bands were not missed due to single-crystal selection rules. Reference spectra of the org. base cations as their bromide salts were also recorded.

---

[2]) The cations employed in compounds **1–11** have been labelled **I–XI** (*Tables 1* and *2*) for convenience. Other compounds studied previously in this project are mentioned in the references, and the cations that were employed have been numbered from **XII** onwards (see *Tables 12–14*).

Table 1. *Cations Used to Generate New Bromothallate(III) Salts in This Work*

	Diethylenetriammonium (**I**)
	N,N,N′,N″,N″-Pentamethyldiethylenetriammonium (**II**)
	Triethylenediammonium (**III**)
	1-Benzylpiperazinium (**IV**)
	Pyrazolinium (**V**)
	1,5-Diazabicyclo[4.3.0]non-5-enium (**VI**)
	Trimethyl(phenyl)ammonium (**VII**)
	(Pyridin-2-yl)-(2-pyridinium)amine (**VIII**)
	1,8-Diazabicyclo[5.4.0]undec-7-enium (**IX**)
	Piperidinium (**X**)
	Quinolinium (**XI**)

2.3. *X-Ray Crystallography.* The crystallographic data for compounds **1–8** are given in *Table 3*[3]). All measurements were conducted at low-temp. on a *Nonius KappaCCD* area-detector diffractometer [10]

---

[3])   CCDC-697489–697496 contain the supplementary crystallographic data for complexes **1–8**. These data can be obtained free of charge from the *Cambridge Crystallographic Data Centre via* www.ccdc.cam.ac.uk/data_request/cif.

Table 2. *Preparative Data for the Bromothallate(III) Complexes*

	Organic cation employed	Solvent	Crystal color/form	Crop	M.p. [°]	Microanalysis [%][a]	Formula
1	Diethylenetriammonium (**I**)	MeOH	Yellow tablet	2nd	187–188	Found: C 6.27, H 1.95, Br 60.52, N 5.32 / Calc.: C 6.08, H 2.04, Br 60.68, N 5.32	$[C_4H_{16}N_3]\cdot[TlBr_6]$
2	N,N,N',N'',N''-Pentamethyl-diethylenetriammonium (**II**)	MeOH	Orange block	2nd	105	Found: C 9.99, H 2.42, Br 55.38, N 3.88 / Calc.: C 10.19, H 2.47, Br 56.47, N 1.98	$[C_9H_{26}N_3]_2\cdot[TlBr_4]_3\cdot 3\ Br$
3	Triethylenediammonium (DABCO) (**III**)	Conc. HBr	Yellow prism	2nd	290	Found: C 10.07, H 1.96, N 3.84 / Calc.: C 10.04, H 1.96, N 3.90	$[C_6H_{14}N_2]\cdot[TlBr_5]$
4	1-Benzylpiperazinium (**IV**)	EtOH	Orange plate	1st	240	Found: C 17.19, H 2.28, Br 51.08, N 3.63 / Calc.: C 16.89, H 2.32, Br 51.08, N 3.58	$[C_{11}H_{18}N_2]\cdot[TlBr_4]\cdot Br$
5	Pyrazolinium (**V**)	Conc. HBr	Orange prism	1st	205	Found: C 8.11, H 0.97, Br 52.80, N 6.23 / Calc.: C 8.10, H 1.13, Br 53.87, N 6.44	$[C_3H_5N_2]_3\cdot[TlBr_4]_2\cdot Br$
6	1,5-Diazabicyclo[4.3.0]non-5-enium (**VI**)	MeOH	Yellow prism	1st	166	Found: C 13.05, H 1.90, Br 49.04, N 4.32 / Calc.: C 12.95, H 2.02, Br 49.23, N 4.31	$[C_7H_{13}N_2]\cdot[TlBr_4]$
7	Trimethylphenylammonium (**VII**)	Conc. HBr	Pale blue prism	2nd	165	Found: C 16.50, H 2.14, Br 48.60, N 2.15 / Calc.: C 16.37, H 2.14, Br 48.41, N 2.12	$[C_9H_{14}N]\cdot[TlBr_4]$
8	(Pyridin-2-yl)-(2-pyridinium)-amine (**VIII**)	MeOH	Yellow prism	1st	266	Found: C 17.24, H 1.38, Br 45.58, N 6.16 / Calc.: C 17.25, H 1.44, Br 45.91, N 6.04	$[C_{10}H_{10}N_3]\cdot[TlBr_4]$
9	1,8-diazabicyclo[5.4.0]undec-7-enium (**IX**)	MeOH	Pale yellow tablet	1st	135	Found: C 16.04, H 2.58, Br 47.06, N 4.21 / Calc.: C 16.83, H 2.54, Br 46.98, N 4.15	$[C_9H_{17}N_2]\cdot[TlBr_4]$
10	Piperidinium (**X**)	Conc. HBr	Yellow needle	1st	66	Found: C 9.64, H 1.90, Br 51.38, N 2.17 / Calc.: C 9.84, H 1.65, Br 51.17, N 2.29	$[C_5H_{12}N]\cdot[TlBr_4]$
11	Quinolinium (**XI**)	Conc. HBr	Orange powder	2nd	160–161	Found: C 15.72, H 1.48, Br 48.55, N 2.07 / Calc.: C 16.52, H 1.23, Br 48.85, N 2.14	$[C_9H_8N]\cdot[TlBr_4]$

[a] Microanalyses were performed by the Campbell Microanalytical Laboratory, University of Otago, New Zealand, and the calculated values are based on the formula shown.

using graphite-monochromated MoK_α radiation (λ 0.71073 Å) and an *Oxford Cryosystems Cryostream 700* cooler. Data reduction was performed with HKL Denzo and Scalepack [11]. The intensities were corrected for *Lorentz* and polarization effects. For **1**, an empirical absorption correction was applied using *SORTAV*, which is based on an analysis of symmetry-equivalent reflections in the highly redundant data set [12]. A numerical absorption correction [13] was applied to each of the remaining data sets. Each structure was solved by direct methods using SIR92 [14], which revealed, at a minimum, the positions of the Tl- and Br-atoms. All remaining non-H-atoms were located in subsequent difference *Fourier* maps.

In **1**, the Tl-atom lies on a center of inversion, while the central N-atom of the cation lies on a C_2 axis. In **6**, the anion sits across a mirror plane with the Tl- and two Br-atoms on the mirror. The cation lies over a crystallographic center of inversion and is, therefore, disordered about this symmetry center. The overlapping disordered orientations of the ions caused instability in the refinement of the atomic positions. Therefore, bond-length restraints were applied to most of the bonds within the cation in order to maintain reasonable geometry. Neighboring atoms within and between each disordered orientation of the cation were also restrained to have similar atomic displacement parameters. Compound **8** contains two symmetry-independent cations, each of which is disordered across a center of inversion. The disorder superimposes inverted copies of the cations upon themselves. This arrangement necessitated defining the amino N-atom in each cation with a site occupation factor of 0.5, while the site for each C-atom adjacent to the amino N-atom, as well as the sites of the pyridinyl and pyridinium N-atoms, are occupied by 0.5C + 0.5N, where the atoms used to define a composite atom site were constrained to have identical fractional coordinates and anisotropic displacement parameters.

The non-H-atoms in each structure were refined anisotropically. For **1**, the H-atom of the central ammonium group of the cation was placed in the position indicated by a difference *Fourier* map, and its position was allowed to refine. The remaining H-atoms, as well as those in each of the other structures, were placed in geometrically calculated positions and constrained to ride on their parent atoms. Each H-atom was assigned an isotropic displacement parameter with a value equal to 1.2 U_{eq} of its parent atom (1.5U_{eq} for Me and $-NH_3^+$ groups). A circular difference *Fourier* map was calculated and used to estimate the orientation of the H-atoms of the symmetry-unique $-NH_3^+$ group in **1** and of the Me groups in **2** and **7**. Although the H-atoms could not be located definitively for **6**, in adding the H-atoms to the model, it was assumed that the cation is protonated at the imine N-atom, N(5). This assumption was supported by the fact that a logical N–H $\cdots$ Br H-bond is evident only if this N-atom is protonated. For **8**, the cations could be protonated at the amino N-atom or at a pyridinyl N-atom, or possibly even disordered between the two pyridinyl N-atoms, but the disorder of the cations made it difficult to locate the positions of these H-atoms definitively. Protonation at any of the possible sites leads to a reasonable arrangement of H-bonds. While refinement of the various alternative models left the *R*-factor virtually unchanged, a test refinement of the isotropic atomic displacement parameters of the amino and pyridinium H-atoms led to reasonable values for these parameters only when the cations were defined as having one amino and one pyridinium H-atom, with the latter not being disordered between the two pyridinyl N-atoms. Also, the amino N–C bond lengths of *ca.* 1.35 Å are shorter than would be expected if the amino group was protonated.

The refinement of each structure was carried out on F^2 using full-matrix least-squares procedures, which minimized the function $\Sigma w(F_o^2 - F_c^2)^2$. Complex **3** crystallizes in a polar space group, and the correct absolute structure has been confirmed by refinement of the absolute structure parameter [15][16], which converged to a value of $-0.016(6)$. Corrections for secondary extinction were applied in each case. For **5**, four reflections, whose intensities were considered to be outliers, were omitted from the final cycles of refinement. For each structure, the largest peaks of residual electron density were always within the vicinity of the Tl- or Br-atoms. The scattering factors for non-H-atoms were taken from [17], and the scattering factors for H-atoms were taken from [18]. For **3**, anomalous dispersion effects were included in F_c [19]; the values for f' and f'' were those from [20]. The values of the mass attenuation coefficients were those from [21]. All calculations were performed using SHELXL97 [22]. The figures were drawn using ORTEPII [23] and the PLUTON routine in the program PLATON [24].

Table 3. *Crystallographic Data for Bromothallate(III) Complexes* **1–8**

	1	**2**	**3**	**4**	**5**	**6**	**7**	**8**
Crystallized from	MeOH	MeOH	conc. HBr	EtOH	conc. HBr	MeOH	conc. HBr	MeOH
Empirical formula	$C_4H_{16}Br_6N_3Tl$	$C_{18}H_{52}Br_{15}N_6Tl_3$	$C_6H_{14}Br_5N_2Tl$	$C_{11}H_{18}Br_5N_2Tl$	$C_9H_{15}Br_9N_6Tl_2$	$C_7H_{13}Br_4N_2Tl$	$C_9H_{14}Br_4N_4Tl$	$C_{10}H_{10}Br_4N_3Tl$
Formula weight [g mol⁻¹]	789.91	2164.1	718.01	782.10	1335.0	649.11	660.13	696.13
Crystal color, habit	yellow, tablet	orange, block	yellow, prism	orange, plate	orange, prism	yellow, prism	pale blue, prism	yellow, prism
Crystal dimensions [mm]	0.13 × 0.18 × 0.25	0.18 × 0.18 × 0.20	0.12 × 0.18 × 0.23	0.02 × 0.07 × 0.15	0.18 × 0.20 × 0.20	0.12 × 0.18 × 0.23	0.15 × 0.18 × 0.23	0.15 × 0.25 × 0.25
Temp. [K]	160(1)	160(1)	160(1)	160(1)	160(1)	160(1)	160(1)	160(1)
Crystal system	orthorhombic	monoclinic	orthorhombic	monoclinic	orthorhombic	monoclinic	monoclinic	monoclinic
Space group	$Pccn$	$P2_1/c$	$P2_12_12_1$	$P2_1/c$	$Pbca$	$P2_1/m$	$P2_1/c$	$P2_1/c$
Z	4	4	4	4	8	2	4	4
Reflections for cell determination	43942	128299	31346	30866	64415	16178	59178	56439
2θ Range for cell determination [°]	4–60	4–55	4–60	4–60	4–60	4–60	4–60	4–60
Unit cell parameters: a [Å]	14.5676(1)	18.8343(1)	8.6889(1)	7.15573(1)	12.9592(1)	6.8059(1)	7.9330(1)	8.5951(1)
b [Å]	7.8893(1)	19.3326(1)	11.5244(1)	14.8364(2)	15.4960(1)	14.9054(3)	14.7228(2)	13.9310(1)
c [Å]	13.8278(1)	14.4876(1)	15.4304(2)	17.8889(3)	27.2931(2)	7.2267(2)	14.0464(2)	13.6033(2)
β [°]	90	105.6794(4)	90	90.5038(6)	90	92.4261(8)	105.8814(5)	95.1579(5)
V [Å³]	1589.20(3)	5078.87(5)	1545.11(3)	1899.52(5)	5480.88(7)	732.45(3)	1577.94(4)	1622.24(3)
$F(000)$	1408	3880	1280	1416	4704	580	1184	1248
D_x [g cm⁻³]	3.301	2.830	3.086	2.735	3.235	2.943	2.779	2.850
$\mu(MoK_\alpha)$ [mm⁻¹]	25.25	21.33	23.38	19.03	24.90	21.92	20.35	19.81
Transmission factors [min; max]	0.030; 0.126	0.048; 0.140	0.034; 0.134	0.116; 0.522	0.026; 0.097	0.050; 0.146	0.042; 0.155	0.038; 0.156
Scan type	ϕ and ω	ϕ and ω	ϕ and ω	ϕ and ω	ω	ϕ and ω	ϕ and ω	ϕ and ω
$2\theta_{(max)}$ [°]	60	55	60	60	60	60	60	60
Reflections measured	38769	111402	47950	46059	89921	19959	73571	79532
Symmetry-independent reflections	2328	11638	4518	5515	7976	2216	4612	4717
R_{int}	0.135	0.096	0.083	0.088	0.144	0.080	0.095	0.089

Table 3 (cont.)

	1	2	3	4	5	6	7	8
Reflections with $I > 2\sigma(I)$	2102	9191	4287	4263	5375	1947	3886	3808
Parameters refined	71	390	128	173	236	110 (69 restraints)	140	173
R (on F; $I > 2\sigma(I)$ reflections)	0.0287	0.0335	0.0232	0.0321	0.0387	0.0291	0.0304	0.0254
wR (on F^2; all indep. refl.)	0.0712	0.0722	0.0524	0.0688	0.0834	0.0650	0.0703	0.0554
Weighting parameters $[a; b]$[a]	0.0270; 3.5015	0.0276; 12.9249	0.0215; 2.4040	0.0276; 1.4652	0.0291; 6.1765	0.0196; 2.5316	0.0071; 9.3679	0.0184; 2.1247
Goodness-of-fit	1.071	1.033	1.047	1.018	1.015	1.049	1.173	1.100
Secondary extinction coefficient	0.0014(1)	0.00023(1)	0.00204(8)	0.00050(7)	0.00019(1)	0.0047(3)	0.00160(8)	0.00102(6)
Final Δ_{max}/σ	0.001	0.003	0.002	0.001	0.003	0.001	0.001	0.002
$\Delta\rho$ (max; min) [e Å^{-3}]	1.26; −2.46	1.20; −1.68	1.00; −1.58	1.26; −1.38	1.36; −1.72	1.33; −1.39	1.65; −1.44	1.40; −1.31

[a]) $w^{-1} = \sigma^2(F_o^2) + (aP)^2 + bP$ where $P = (F_o^2 + 2F_c^2)/3$.

3. Results and Discussion. – 3.1. *Salts with Trivalent Cations.* The diethylenetriammonium (**I**) and *N,N,N′,N″,N″*-pentamethyldiethylenetriammonium (**II**) cations provide an extension of the open-chain alkyl diammonium series [2] and are interesting, because they are the first trivalent cations employed in these investigations. In addition, it was anticipated that such large cations would stabilize a similarly large counter-anion with equal but opposite charge, in accordance with *Basolo*'s generalization [25].

Indeed, for the complex **1** with $[C_4H_{16}N_3] \cdot [TlBr_6]$ stoichiometry, the X-ray crystallography revealed the presence of discrete $[C_4H_{16}N_3]^{3+}$ cations and $[TlBr_6]^{3-}$ anions (*Fig. 1*). The cation has crystallographic C_2 symmetry about the central N-atom and the anion lies on a center of inversion. The anion deviates somewhat from perfect octahedral geometry in that it is squashed along one axis, with these Tl−Br bonds being *ca.* 0.19 Å shorter than the remaining Tl−Br bonds (*Table 4*). A similar Tl−Br bond shortening of *ca.* 0.18 Å was observed along one axis of the C_i-symmetric octahedral $[TlBr_6]^{3-}$ anion in the *N,N*-diethylpropane-1,3-diammonium cation (**XII**) mixed salt [2]. Mixed salts containing $[TlBr_6]^{3-}$ anions have also been found in the complexes involving the 1,1,3,3-tetramethylimidazolidinium and hexane-1,5-diammonium cations (**XIII** and **XIV**, resp.) [2][4], but the distortions of the octahedra were minimal, with the anions possessing S_4 and S_6 symmetry, respectively. Compound **1** is unique in that it is the first example of a bromothallate(III) salt with an organic base cation in which a $[TlBr_6]^{3-}$ anion is present as the sole anionic species.
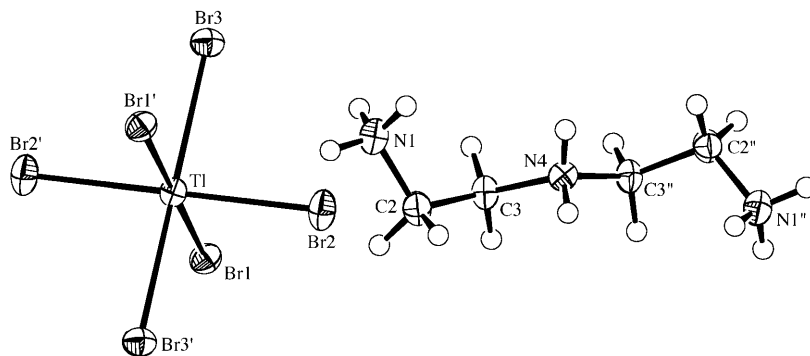

Fig. 1. *The components in the structure of $[C_4H_{16}N_3] \cdot [TlBr_6]$* (**1**) *showing the atom-labeling scheme and 50% probability for the displacement ellipsoids.* The labels with ′ and ″ indicate atoms generated from the unique atoms by the inversion and C_2 symmetry, respectively.

The ions in **1** are linked by a complex three-dimensional network of N−H⋯Br H-bonds with each cation affording eight potential H-bond donors (*Table 5* and *Fig. 2*). Each of the H-atoms of the central amine group interacts with a different $[TlBr_6]^{3-}$ anion, and each H-atom forms bifurcated H-bonds with two different Br-atoms from the same anion. For the symmetry-unique terminal amine group, one of the H-atoms forms trifurcated H-bonds, although two of them are quite weak. The corresponding acceptor Br-atoms all come from the same anion, but this anion is not one of the anions that interact with the central N-atom. The other two H-atoms of the termnal amine

Table 4. *Selected Interatomic Distances [Å] and Angles [°] for [C₄H₁₆N₃]·[TlBr₆] (**1**) and [C₉H₂₆N₃]₂·* *[TlBr₄]₃·3 Br (**2**), with Standard Uncertainties in Parentheses*[a]

Complex **1**			
Tl−Br(1)	2.8064(4)	Tl−Br(3)	2.7872(4)
Tl−Br(2)	2.6616(4)		
Br(1)−Tl−Br(1)ⁱ	180	Br(1)−Tl−Br(2)	89.32(1)
Br(2)−Tl−Br(2)ⁱ	180	Br(1)−Tl−Br(3)	89.36(1)
Br(3)−Tl−Br(3)ⁱ	180	Br(2)−Tl−Br(3)	89.72(1)
Complex **2**			
Tl(1)−Br(4)	2.5337(7)	Tl(2)−Br(10)	2.5727(7)
Tl(1)−Br(5)	2.5821(6)	Tl(2)−Br(11)	2.5406(7)
Tl(1)−Br(6)	2.5544(7)	Tl(3)−Br(12)	2.5570(7)
Tl(1)−Br(7)	2.5365(7)	Tl(3)−Br(13)	2.5402(7)
Tl(2)−Br(8)	2.5549(7)	Tl(3)−Br(14)	2.5701(7)
Tl(2)−Br(9)	2.5497(7)	Tl(3)−Br(15)	2.5300(7)
Br(4)−Tl(1)−Br(5)	107.73(2)	Br(9)−Tl(2)−Br(10)	105.72(2)
Br(4)−Tl(1)−Br(6)	115.68(3)	Br(9)−Tl(2)−Br(11)	115.08(2)
Br(4)−Tl(1)−Br(7)	110.06(3)	Br(10)−Tl(2)−Br(11)	106.77(2)
Br(5)−Tl(1)−Br(6)	103.89(2)	Br(12)−Tl(3)−Br(13)	114.14(2)
Br(5)−Tl(1)−Br(7)	108.86(2)	Br(12)−Tl(3)−Br(14)	107.31(2)
Br(6)−Tl(1)−Br(7)	110.24(3)	Br(12)−Tl(3)−Br(15)	103.15(2)
Br(8)−Tl(2)−Br(9)	108.03(2)	Br(13)−Tl(3)−Br(14)	105.15(2)
Br(8)−Tl(2)−Br(10)	108.53(2)	Br(13)−Tl(3)−Br(15)	116.95(3)
Br(8)−Tl(2)−Br(11)	112.34(2)	Br(14)−Tl(3)−Br(15)	109.85(3)

[a]) Symmetry operator: ⁱ $1-x$, $-y$, $1-z$.

group each interact singly with additional [TlBr₆]³⁻ anions, one of which is one of the anions involved with one of the central amine H-atoms. The other terminal amine group, being related to the first by the C_2 axis of the cation, has an identical set of interactions with symmetry-related anions. The interactions result in each ion being H-bonded to six different counter-ions. Two of the three symmetry-independent Br-atoms of the [TlBr₆]³⁻ anion each accept three H-bonds. The Br-atom of the shorter Tl−Br bond only accepts one H-bond, which is presumably the reason that this Br-atom forms the shortest Tl−Br bond. This geometry is consistent with the previously discussed observation [2] that the shortest Tl−Br bonds in the [TlBr₆]³⁻ anions of the mixed salts from cations **XII** and **XIV** always involve the Br-atoms that accept the fewest, if any, H-bonds of any of the Br-atoms in these anions. By contrast, the quaternized cation **XIII** precludes any H-bonding, and the Tl−Br bond lengths in the [TlBr₆]³⁻ anion of its bromothallate(III) mixed salt are all found to be equal by symmetry [4]. This observation further supports the hypothesis mentioned earlier [2] that the N−H⋯Br H-bonding interactions are extracting the acceptor Br-atom from the Tl-atom by decreasing the available electron density on that Br-atom, thus weakening the coordination strength of the Br-atom and producing a slightly longer Tl−Br bond.

The *Raman* spectrum of **1** shows three peaks at 161, 153, and 95 cm⁻¹, which have been assigned to the $\nu_1(A_{1g})$, $\nu_2(E_g)$, and $\nu_5(F_{2g})$ modes, respectively, expected for an
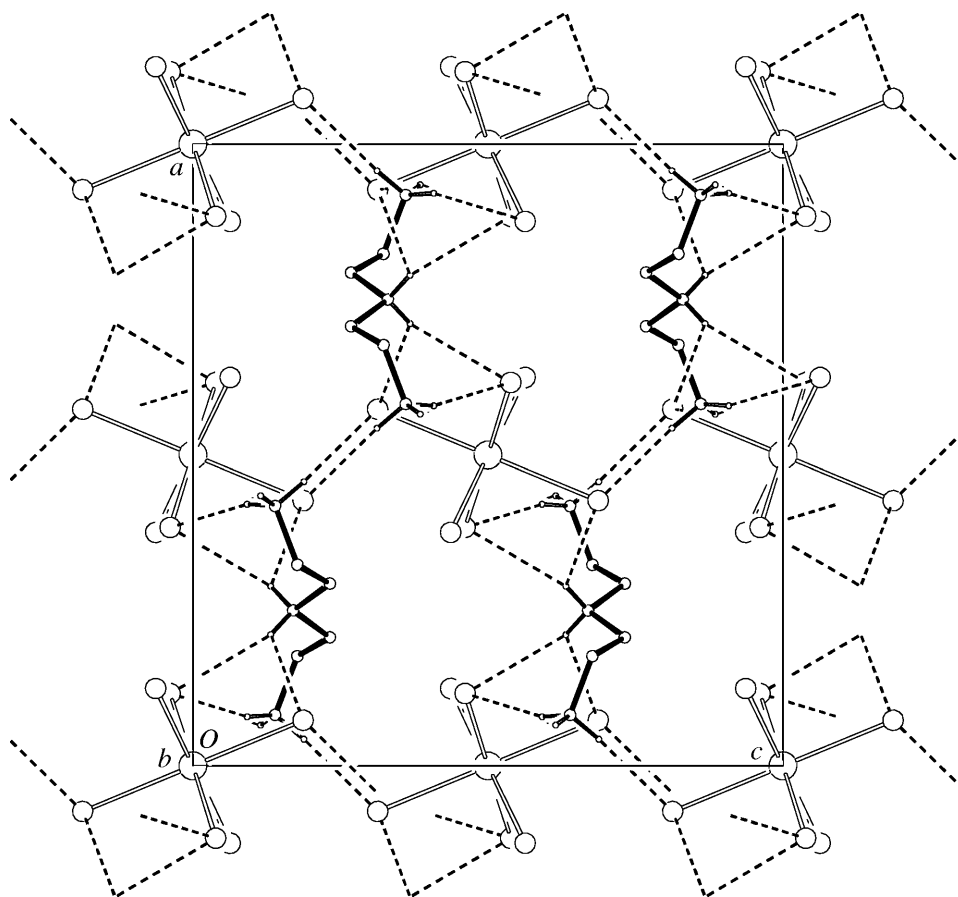
Fig. 2. *A projection of the crystal packing of* **1** *viewed down [0 1 0] showing the H-bonding as dashed lines. The H-atoms bonded to C-atoms have been omitted for clarity.*

octahedral $[TlBr_6]^{3-}$ unit. These bands are consistent with those tentatively assigned to the $[TlBr_6]^{3-}$ anion in the other mixed salts (cations **XII**, **XIII**, and **XIV**), although it has to be borne in mind that those salts also incorporated $[TlBr_4]^-$ ions [2][4]. Unfortunately, a comparison spectrum from a well-characterized $[TlBr_6]^{3-}$ complex is not available in the literature. While these assignments are similar to those made for $Rb_3TlBr_6 \cdot {}^8/_7 H_2O$, the spectrum of the Rb salt and that of $K_3TlCl_6 \cdot H_2O$ are more complex than expected [26]. In the latter case, the crystal structure is reported to contain one $[TlCl_5 \cdot H_2O]^{2-}$ and two $[TlCl_6]^{3-}$ units, which give rise to two *Raman* lines [27]. Only preliminary results for the structure of hydrated rubidium hexabromothallate(III) have ever appeared [28], and it is possible that similar halide/H_2O ligand exchange also occurs in that salt and affects the spectrum.

In contrast to **1**, the quite similar *N,N,N′,N″,N″*-pentamethyldiethylenetriammonium cation (**II**) generates a bromothallate(III) **2**, with $[C_9H_{26}N_3]_2 \cdot [TlBr_5]_3$ stoichiometry, whereas the crystal structure reveals a mixed salt containing discrete $[TlBr_4]^-$

Table 5. *H-Bonding Parameters for $[C_4H_{16}N_3]\cdot[TlBr_6]$* (**1**) *and $[C_9H_{26}N_3]_2\cdot[TlBr_4]_3\cdot3\ Br$* (**2**), *with Standard Uncertainties in Parentheses*

$D-H\cdots A$[a]	$D-H$ [Å]	$H\cdots A$ [Å]	$D\cdots A$ [Å]	$D-H\cdots A$ [°]
Complex **1**				
$N(1)-H(11)\cdots Br(1)$	0.91	2.82	3.514(4)	134
$N(1)-H(11)\cdots Br(2)$	0.91	2.88	3.510(4)	128
$N(1)-H(11)\cdots Br(3)$	0.91	2.94	3.560(4)	126
$N(1)-H(12)\cdots Br(1)^{i}$	0.91	2.44	3.339(4)	171
$N(1)-H(13)\cdots Br(3)^{ii}$	0.91	2.36	3.242(4)	163
$N(4)-H(4)\cdots Br(1)^{iii}$	0.88(4)	2.79(4)	3.4027(5)	128(4)
$N(4)-H(4)\cdots Br(3)^{iv}$	0.88(4)	2.80(5)	3.483(4)	136(4)
Complex **2**				
$N(1)-H(1)\cdots Br(2)^{v}$	0.93	2.31	3.227(5)	167
$N(4)-H(4)\cdots Br(1)$	0.93	2.37	3.280(5)	167
$N(7)-H(7)\cdots Br(1)^{vi}$	0.93	2.34	3.250(5)	166
$N(13)-H(13)\cdots Br(3)$	0.93	2.47	3.332(5)	154
$N(16)-H(16)\cdots Br(3)$	0.93	2.26	3.184(5)	175
$N(19)-H(19)\cdots Br(2)$	0.93	2.32	3.222(5)	163

[a]) Symmetry operators: [i] $1-x$, $1/2+y$, $3/2-z$; [ii] $1-x$, $1-y$, $1-z$; [iii] $1/2-x$, $1/2-y$, z; [iv] $x-1/2$, $1/2+y$, $1-z$; [v] $1-x$, $2-y$, $1-z$; [vi] $-x$, $2-y$, $1-z$.

and Br^- anions (*Fig. 3*). The asymmetric unit in the structure contains two cations, three $[TlBr_4]^-$ anions, and three Br^- ions, with none of these entities occupying any special symmetry sites. There are no $Tl\cdots$ bromide-ion distances shorter than 5.7 Å, which precludes any weak interactions between the $[TlBr_4]^-$ and Br^- ions. The shortest interionic $Tl\cdots Br$ distance of 4.2104(7) Å is between two $[TlBr_4]^-$ anions and is marginally inside the accepted value of *ca.* 4.3 Å for the sum of the *Van der Waals* radii of the Tl- and Br-atoms [29]. This interaction involves $Tl(2)-Br(9)\cdots Tl(3)$. Indeed, as shown in *Table 4*, the distortions of the $[TlBr_4]^-$ anions from ideal tetrahedral geometry are minimal, but greatest for the $[TlBr_4]^-$ anion involving the atom $Tl(3)$, which is consistent with a small influence of the atom $Br(9)$ on the geometry of this anion. If this interaction is taken as significant, the two anions involved could be described as a $[Tl_2Br_8]^{2-}$ unit, and the overall structure would then have the formulation $[C_9H_{26}N_3]_2\cdot[Tl_2Br_8]\cdot[TlBr_4]\cdot3\ Br$. However, given that the $Tl(2)-Br(9)\cdots Tl(3)$ angle is quite sharp at 124°, and the proximity of the $Tl(3)\cdots Br(9)$ distance to the *Van der Waals* limit, it is doubtful that this arrangement of the $[TlBr_4]^-$ anions represents the presence of true interactions in the form of $Tl\cdots Br$ secondary bonding [30][31].

All of the potential donor H-atoms of the cations in **2** are involved in $N-H\cdots Br$ H-bonding interactions, and the acceptors are always the isolated Br^- anions (*Table 5*). The cations and Br^- anions intertwine themselves into columns which run parallel to the [1 0 1] direction. All of the $N-H$ groups point towards the center of the column, and the Br^- anions occupy the core of the column (*Fig. 4*). Within the columns, the H-bonds do not form continuous chains, but any one set of interactions is limited to a finite segment of the column. Each segment is composed of four cations and six Br^- anions involving two sets of all symmetry-independent constituent moieties arranged about a center of inversion. The segment starts with cation **B** ($N(13)$, $N(16)$, and $N(19)$), which
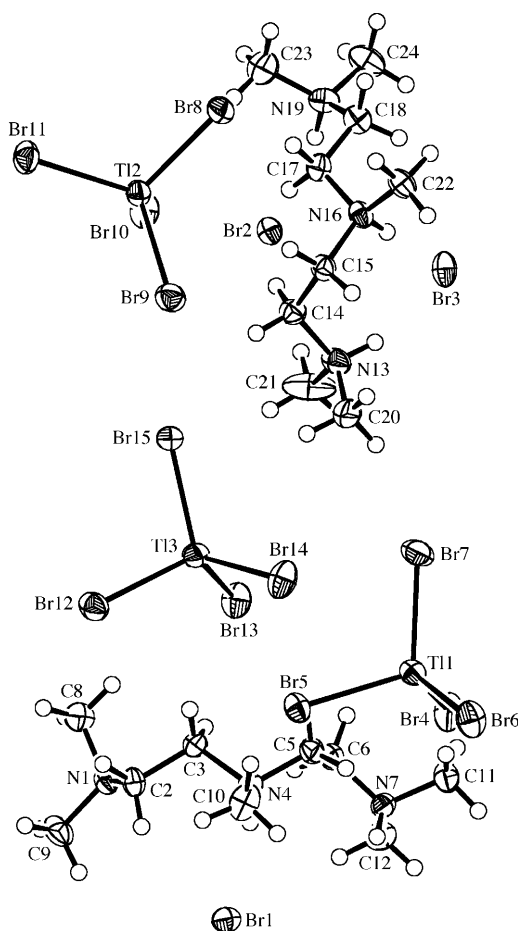
Fig. 3. *The asymmetric unit in the structure of [C$_9$H$_{26}$N$_3$]$_2$·[TlBr$_4$]$_3$·3 Br (**2**) showing the atom-labeling scheme and 50% probability for the displacement ellipsoids*

forms two H-bonding interactions with the same Br$^-$ ion, Br(3). The third interaction from cation **B** is with a different Br$^-$ ion, Br(2), which also accepts a H-bond from one end of cation **A** (N(1), N(4), and N(7)). Thus, Br(2) is bridging between cations **A** and **B**. The remaining two donors in cation **A** each form a H-bond with different symmetry-related Br(1) ions. These anions are related by a center of inversion and, therefore, each accepts two H-bonds from symmetry-related **A** cations. Thus, two Br(1) anions bridge between two cations of type **A**. Because of the center of inversion, this second cation **A** is further connected to another cation **B**, whereupon the segment ends exactly as it began. The H-bonded segment can thus be depicted schematically as shown in *Fig. 5* and represented in the packing diagram displayed in *Fig. 6*.

Mixed salts containing essentially discrete [TlBr$_4$]$^-$ and Br$^-$ ions in various ratios have also been found in the salts from 1,10-phenanthrolinium (**XV**) [5], the pyridinium-based species, 4,4′-dimethyl-2,2′-bipyridinium, pyridinium, and 2-bromo-
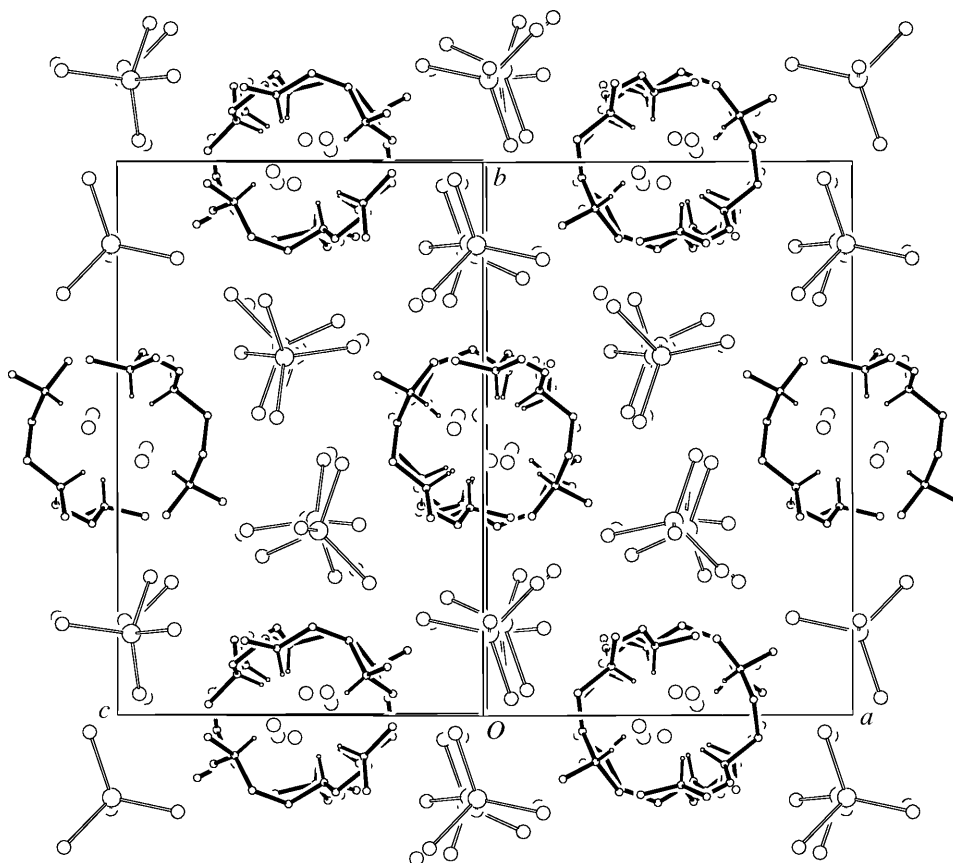
Fig. 4. *A projection of the crystal packing of* **2** *viewed down [1 0 1] showing the columns of cations wrapped around the Br⁻ ions at their core.* These columns are then interspersed by columns of [TlBr₄]²⁻ anions. The H-atoms bonded to C-atoms have been omitted for clarity.

pyridinium (**XVI**, **XVII**, and **XVIII**, resp.) [1][5], and the alkyl cations, *N,N,N′,N′*-tetramethylpropane-1,3-diammonium and *N,N,N′,N′*-tetraethylethylene-1,2-diammonium (**XIX** and **XX**, resp.) [2]. In all these, as in **2**, the [TlBr₄]⁻ anions never act as acceptors of H-bonds, these interactions being restricted to the Br⁻ ions. An exception is the pyrazolinium salt (**5**; *vide infra*), which also contains discrete [TlBr₄]⁻ and Br⁻ ions, but both species act as acceptors of H-bonds.

Having obtained a [TlBr₆]³⁻ anion with the trivalent diethylenetriammonium cation in **1**, as predicted by *Basolo*'s generalization [25], it might reasonably be expected that the closely related trivalent cation **II** should also yield a complex in which [TlBr₆]³⁻ anions are present. That the mixed salt, **2**, without any [TlBr₆]³⁻ anions, was obtained instead, might be attributed to the larger size of the latter cation caused by the five additional Me substituents. Whereas the relative sizes of the cation and anion in **1** apparently allow the ions to pack comfortably in a 1 : 1 ratio to give a cation/Tl/Br ratio of 1 : 1 : 6, the larger cation in **2** must be less compatible with the size of the [TlBr₆]³⁻
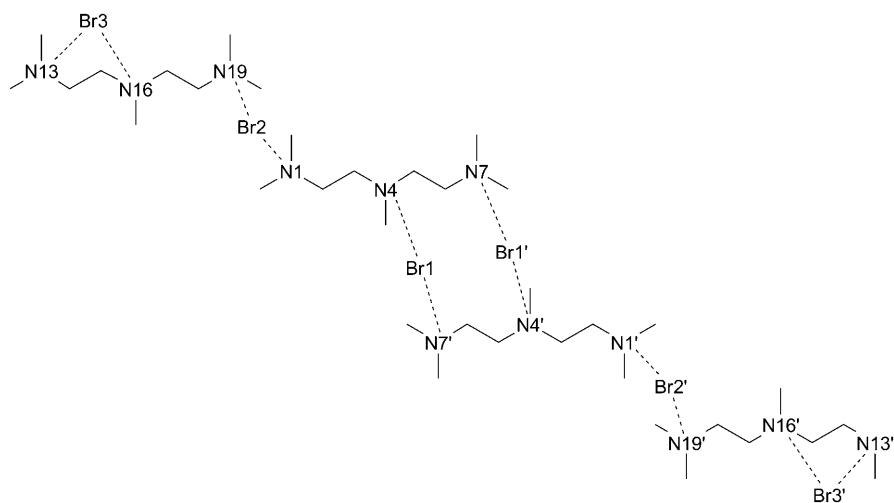
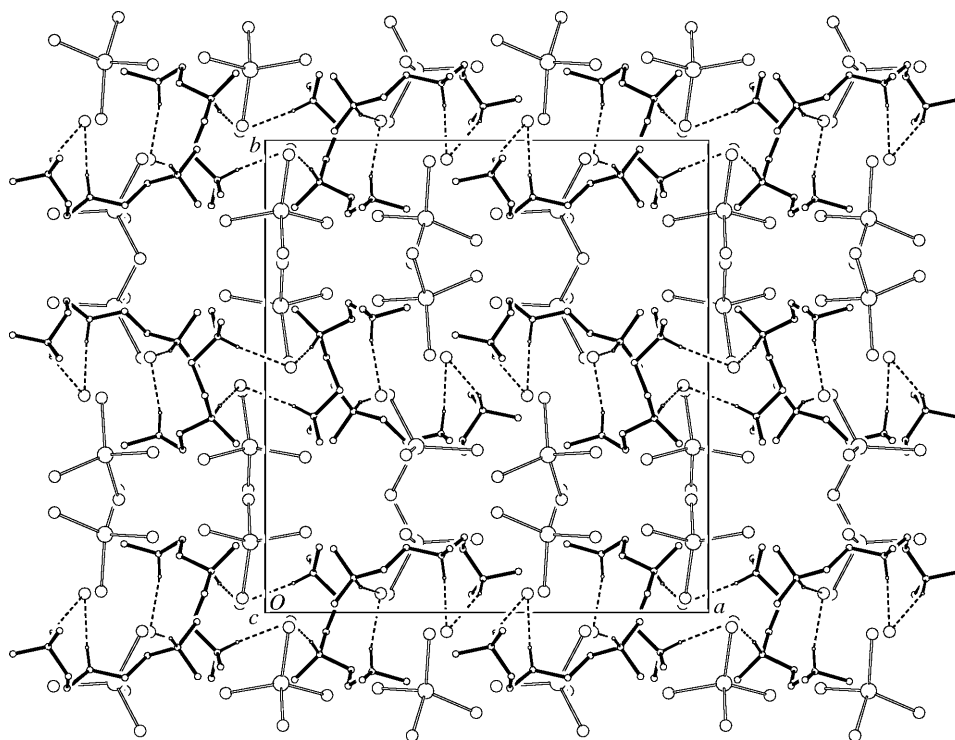Fig. 5. *Schematic of the discrete H-bonded segment in* **2**

Fig. 6. *A projection of the crystal packing of* **2** *viewed down [0 0 1] showing the H-bonding as dashed lines.* Three horizontal columns of cations and Br⁻ ions are shown, and each contains two discrete H-bonded segments. The H-atoms bonded to C-atoms have been omitted for clarity.

anion, so the anionic arrangement expands into one that requires more volume, but still maintains the required charge balance. This requirement is achieved with the $[C_9H_{26}N_3]_2 \cdot [TlBr_4]_3 \cdot 3\,Br$ stoichiometry in **2**, which has a cation/Tl/Br ratio of $2:3:15$.

3.2. *Salts with Divalent Cations*. The triethylenediammonium (DABCO) cation (**III**) stabilizes a bromothallate(III) salt **3**, with the $[C_6H_{14}N_2] \cdot [TlBr_5]$ stoichiometry. In the crystal structure, the asymmetric unit contains one cation and a highly distorted trigonal bipyramidal $[TlBr_5]^{2-}$ anion with one very long axial $Tl \cdots Br$ distance of 3.6252(5) Å (*Fig. 7*). This geometry can effectively be described as being derived from the distortion of a tetrahedral $[TlBr_4]^-$ unit by the close approach or secondary bonding [30][31] of the fifth Br-atom. The Tl−Br bonds involving atoms Br(3), Br(4), and Br(5), which would be equatorial in a symmetrical trigonal-bipyramidal ion, are bent at the metal atom away from atom Br(2) towards the more distant Br(1)-atom (*Table 6*). The distances of the Tl-, Br(1)- and Br(2)-atoms from the least-squares equatorial plane defined by Br(3), Br(4), and Br(5) are 0.5872(3), − 3.0324(6), and 3.1965(6) Å, respectively. Thus, the two axial Br-atoms are almost equidistant from the equatorial plane, and all five Br-atoms clearly belong to the one trigonal-bipyramidal anionic unit in which the Tl-atom is displaced significantly towards one of the axial Br-atoms. The Tl−Br(2) bond, which is *trans* to the long interaction (Br(1)$\cdots$Tl−Br(2) 175.09(2)°), is only 0.06 Å longer than the equatorial Tl−Br bonds. Secondary bonding between Br⁻ ions and Tl^{III} to give very similar axially distorted trigonal bipyramidal $[TlBr_5]^{2-}$ anions with long $Tl \cdots Br$ distances of *ca.* 3.77 Å has been found in the structures of the piperazinium (**XXI**) and 2,2′-bipyridinium (**XXII**) salts [5], and a slightly shorter $Tl \cdots Br$ distance of 3.40 Å is present in the $[TlBr_5]^{2-}$ anion of the 2-(ammoniomethyl)pyridinium (**XXIII**) salt [1]. These contrast with the more regular trigonal bipyramidal $[TlBr_5]^{2-}$ species (longest Tl−Br 2.73–2.92 Å) found in the structures of the *N,N′*-diethyl-*N,N,N′,N′*-tetramethylethylene-1,2-diammonium (**XXIV**) [2] and *N,N′*-diethyltriethylenediammonium (diethyl-DABCO; **XXV**) salts [4] and in both polymorphs of the 1,1,4,4-tetramethylpiperazinium (**XXVI**) compound [4][6].
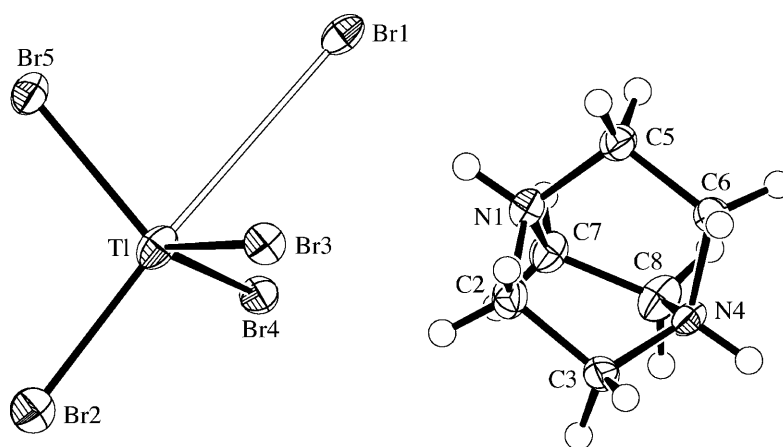

Fig. 7. *The asymmetric unit in the structure of $[C_6H_{14}N_2] \cdot [TlBr_5]$ (**3**) showing the atom-labeling scheme and highlighting the long secondary $Tl \cdots Br(1)$ bond of 3.6252(5) Å. The displacement ellipsoids are shown at the 50% probability level.*

Table 6. *Selected Interatomic Distances* [Å] *and Angles* [°] *for [C₆H₁₄N₂]·[TlBr₅]* (**3**) *and [C₁₁H₁₈N₂]·* *[TlBr₄]·Br* (**4**), *with Standard Uncertainties in Parentheses*

	3	**4**
Tl–Br(1)	3.6252(5)	4.0224(5)
Tl–Br(2)	2.6123(6)	2.5980(5)
Tl–Br(3)	2.5429(5)	2.5173(5)
Tl–Br(4)	2.5532(4)	2.5496(5)
Tl–Br(5)	2.5537(5)	2.5713(5)
Br(1)–Tl–Br(2)	175.09(2)	172.41(1)
Br(1)–Tl–Br(3)	75.89(1)	77.85(1)
Br(1)–Tl–Br(4)	74.46(1)	68.92(1)
Br(1)–Tl–Br(5)	79.78(1)	78.07(1)
Br(2)–Tl–Br(3)	105.58(2)	108.76(2)
Br(2)–Tl–Br(4)	100.78(2)	104.33(2)
Br(2)–Tl–Br(5)	103.54(2)	102.06(2)
Br(3)–Tl–Br(4)	115.61(2)	115.00(2)
Br(3)–Tl–Br(5)	114.84(2)	113.27(2)
Br(4)–Tl–Br(5)	114.14(2)	112.11(2)

Each cation in **3** forms strong N–H⋯Br H-bonds with only the weakly bound axial Br-atom of two different [TlBr₅]²⁻ anions, and this Br-atom, in turn, accepts H-bonds from two different cations (*Table 7*). The H-bonds link the cations and anions into continuous chains which run parallel to the [010] direction in the sequence: ⋯ (cation)→Br⁻←(cation)→Br⁻⋯ (*Fig. 8*). This H-bonding pattern can be described by the graph set motif [32] of $C_2^1(7)$. Interestingly, although no chiral moieties are present, **3** crystallizes in a polar space group, as did the complex from cation **XXV** [4], and the absolute structure has been determined by refinement of the absolute structure parameter [15][16], which converged to a value of −0.016(6).

The 1-benzylpiperazinium cation (**IV**) stabilizes a bromothallate(III) salt **4**, with the $[C_{11}H_{18}N_2]·[TlBr_5]$ stoichiometry. The asymmetric unit in the crystal structure

Table 7. *H-Bonding Parameters for [C₆H₁₄N₂]·[TlBr₅]* (**3**) *and [C₁₁H₁₈N₂]·[TlBr₄]·Br* (**4**), *with Standard Uncertainties in Parentheses*

D–H⋯Aᵃ)	D–H [Å]	H⋯A [Å]	D⋯A [Å]	D–H⋯A [°]
Complex **3**				
N(1)–H(1)⋯Br(1)	0.93	2.32	3.226(4)	164
N(4)–H(4)⋯Br(1)ⁱ	0.93	2.39	3.238(4)	152
Complex **4**				
N(1)–H(1)⋯Br(1)ⁱⁱ	0.93	2.40	3.296(3)	161
N(4)–H(41)⋯Br(1)	0.92	2.63	3.344(4)	135
N(4)–H(42)⋯Br(1)ⁱⁱⁱ	0.92	2.38	3.248(4)	157
N(4)–H(41)⋯Br(5)ⁱⁱⁱ	0.92	2.87	3.393(4)	117

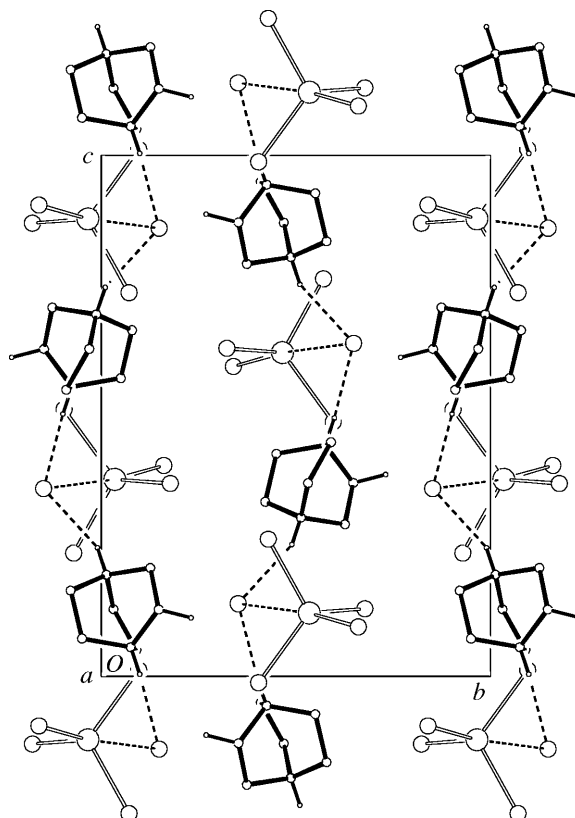ᵃ) Symmetry operators: ⁱ 3/₂ − x, 1 − y, z − ¹/₂; ⁱⁱ x − 1, y, z; ⁱⁱⁱ 1 − x, 1 − y, 1 − z.

Fig. 8. *A projection of the crystal packing of* **3** *viewed down [100] showing the H-bonding as dashed lines.*
The H-atoms bonded to C-atoms have been omitted for clarity.

contains one divalent cation, and one each of almost discrete $[TlBr_4]^-$ and Br^- anions, with none of these entities occupying any special symmetry sites. The anionic species are associated very weakly and could be considered to have an arrangement somewhere between the completely discrete $[TlBr_4]^-$ and Br^- entities found in **2**, and the closer $[TlBr_4] \cdots Br$ association *via* secondary bonding to give the distorted $[TlBr_5]^{2-}$ anion found in **3**. The Br^- ion in **4**, $Br(1)$, lies 4.0224(4) Å from the Tl-atom and is, therefore, just inside the sum of the *Van der Waals* radii for these two atoms (*Fig. 9*). The very slight distortion of the tetrahedral geometry of the $[TlBr_4]^-$ anion is consistent with the influence caused by a very weak interaction between the $[TlBr_4]^-$ anion and the Br^- ion (*Table 6*). The Br^- ion is correctly positioned to be considered as forming the distant apex of a distorted $[TlBr_5]^{2-}$ trigonal bipyramid, as it is nearly *trans* to $Br(2)$ with a $Br(1) \cdots Tl-Br(2)$ angle of 172.41(1)°, and the $Tl-Br(2)$ bond is correspondingly marginally longer than the other three Tl−Br bonds. Although the $[TlBr_4]^-$ anion is distorted only minimally from ideal tetrahedral geometry, the tetrahedral angles are distorted such that all angles involving the $Br(2)$-atom have become smaller than the ideal tetrahedral value, while all angles not involving $Br(2)$ are

slightly larger. The distances of the Tl-, Br(1)-, and Br(2)-atoms from the least-squares plane defined by the pseudo-equatorial atoms, Br(3), Br(4), and Br(5), are 0.6633(3), − 3.3370(5), and 3.2558(5) Å, respectively. Thus, the two pseudo-axial Br-atoms are almost equidistant from the equatorial plane, as found in compound **3**, which further suggests that all five Br-atoms belong to the one anionic unit. All of these features are consistent with the notion that the Br⁻ ion is interacting very slightly with the Tl-atom and distorting the [TlBr₄]⁻ tetrahedron towards a [TlBr₅]²⁻ trigonal bipyramid. A similar arrangement of anions to that in compound **4** was found in the 2-bromopyridinium (**XVIII**) salt, where the Br⁻ ion is 4.1546(6) Å from the Tl-atom, and the [TlBr₄]⁻ tetrahedron is also distorted very slightly [1]. In this latter case, the distances of the Tl- and the two pseudo-axial Br-atoms from the least-squares equatorial plane defined by the pseudo-equatorial Br-atoms are 0.6777(3), − 3.3728(6), and 3.2551(5) Å, respectively, which are very similar to the corresponding distances in compound **4**. Thus, **4** and the 2-bromopyridinium (**XVIII**) salt may be considered to be extreme examples of the weak [TlBr₄]···Br secondary bonding found in **3**, and in the compounds from cations **XXI**, **XXII**, and **XXIII** that were described earlier [1][5].
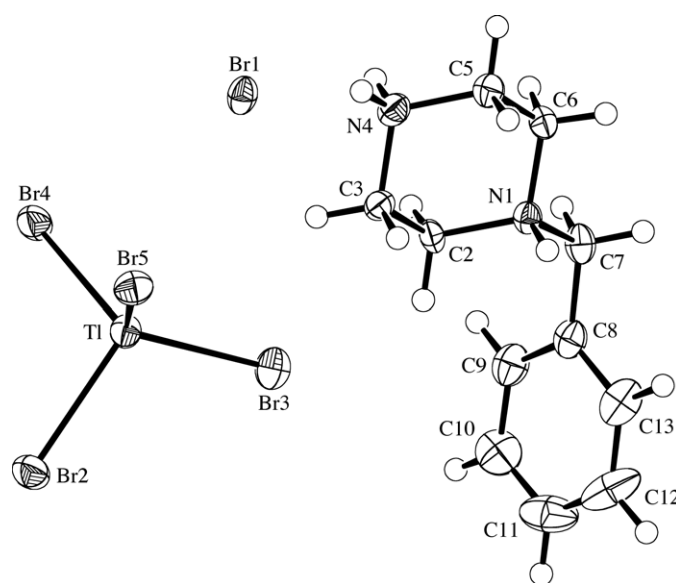
Fig. 9. *The asymmetric unit in the structure of [C₁₁H₁₈N₂]·[TlBr₄]·Br (**4**) showing the atom-labeling scheme and 50% probability for the displacement ellipsoids.* The Tl···Br(1) distance is 4.0224(4) Å.

All three of the potential donor H-atoms of the cation in **4** are involved in N−H··· Br H-bonding interactions with neighboring Br⁻ ions. One H-atom forms bifurcated H-bonds, with the second, weaker interaction being with a Br-atom from the [TlBr₄]⁻ anion (*Table 7*). This latter interaction has a long H···Br distance and a quite acute N−H···Br angle, so is possibly an insignificant interaction. Thus, each cation interacts with three different Br⁻ ions and one [TlBr₄]⁻ anion, while each Br⁻ ion interacts with three different cations. The cation···Br⁻-ion interactions link these ions into

continuous columns, which run parallel to the [1̄00] direction. The construction of the columns can be thought of as a ladder, whose junctions between the rungs and vertical supports are, alternately, a cation and a Br⁻ ion, and each rung has a cation at one end and a Br⁻ ion at the other end (*Fig. 10*). The repeating unit within the columns thus consists of two rungs, **A** and **B**, of the ladder. The rung **A** to rung **B** step consists of two cations and two Br⁻ ions distributed about a center of inversion and involves both of the H-atoms on the unsubstituted N-atom of the cation. The two Br⁻ ions bridge the two cations, and *vice versa*, thus forming a four-membered H-bonded ···cation···Br⁻··· cation···Br⁻··· loop, which has a binary graph set motif [32] of $R_4^2(8)$. The next rung **B** to rung **A** connection is also a centrosymmetric ···cation···Br⁻···cation···Br⁻··· loop, which involves one of the interactions in the first loop plus the third H-bond to each Br⁻ ion, which involves the single H-atom on the benzyl-substituted N-atom of the cation. This latter loop has a binary graph set motif of $R_4^2(14)$.
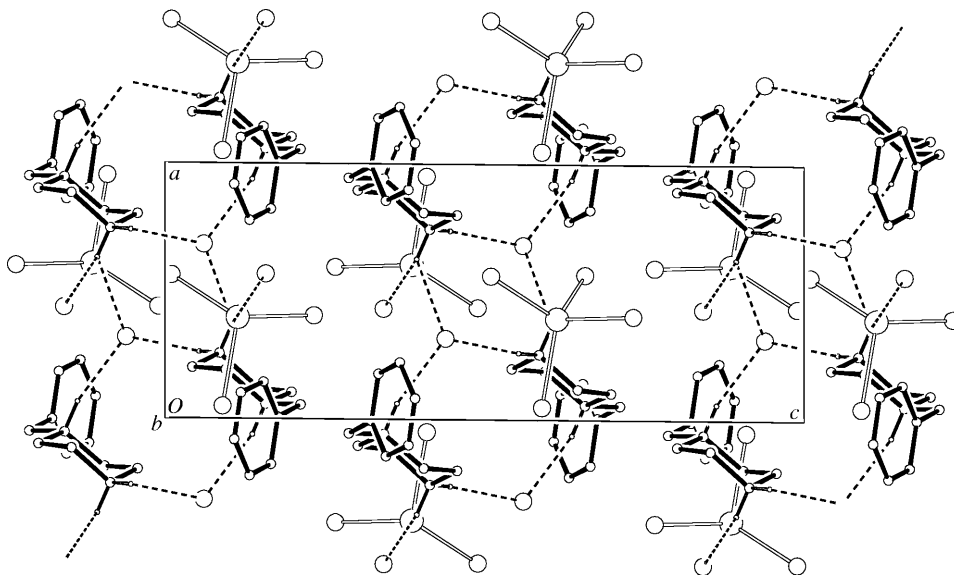
Fig. 10. *A projection of the crystal packing of* **4** *viewed down [010] showing the H-bonding as dashed lines.* The H-atoms bonded to C-atoms have been omitted for clarity.

Compounds **3** and **4** are further examples of the $[TlBr_5]^{2-}$ anion being highly distorted when it is involved in H-bonding interactions with the cation, particularly when these interactions are predominantly with a single Br-atom, which then interacts much less strongly with the Tl-atom. These very weak Tl···Br interactions, or even structures with essentially discrete $[TlBr_4]^-$ and Br⁻ ions, have been found to occur consistently in the presence of cations with N−H H-bond donors, whereas the much more regular $[TlBr_5]^{2-}$ anions are obtained only in the absence of N−H H-bond donors, such as with quaternary organoammonium cations. This hypothesis, first introduced in [1][2], will be discussed later.

3.3. *Salts with Monovalent Cations.* The pyrazolinium cation (**V**) yields a bromothallate(III) salt **5** with the $[Tl_2Br_9]^{3-}$ stoichiometry, but the crystal structure

shows that a formal dinuclear $[Tl_2Br_9]^{3-}$ species is not present. Instead, the asymmetric unit of **5** contains three symmetry-independent pyrazolinium cations, two $[TlBr_4]^-$ anions, and a Br^- ion (*Fig. 11*). The structure is very similar to that found when the pyridinium cation (**XVII**) was employed [1], with the same relative arrangement of cations and anions, a pseudo-$[Tl_2Br_9]^{3-}$ grouping, similar unit cell dimensions, and the same space group. The two structures could be described as pseudo-isostructural, with the different cations precluding true isostructurality. In **5**, the Br^- ion, Br(9), is positioned between the two $[TlBr_4]^-$ anions with a $Tl(1)\cdots Br(9)\cdots Tl(2)$ angle of $111.17(2)°$, and is virtually *trans* to Br(1) in one $[TlBr_4]^-$ anion and Br(8) in the other (*Table 8*). Although this resembles a $[Tl_2Br_9]^{3-}$ grouping, the Br^- ion is 4.7923(8) and 4.4712(8) Å from atoms Tl(1) and Tl(2), respectively, which is similar to the corresponding distances in the pyridinium salt. These distances, being longer than the sum of the *Van der Waals* radii of the Tl- and Br-atoms [29], are too long for any significant interaction between the Br^- and $[TlBr_4]^-$ anions. This conclusion is supported by the minimal distortions of the $[TlBr_4]^-$ anions from ideal tetrahedral geometry.

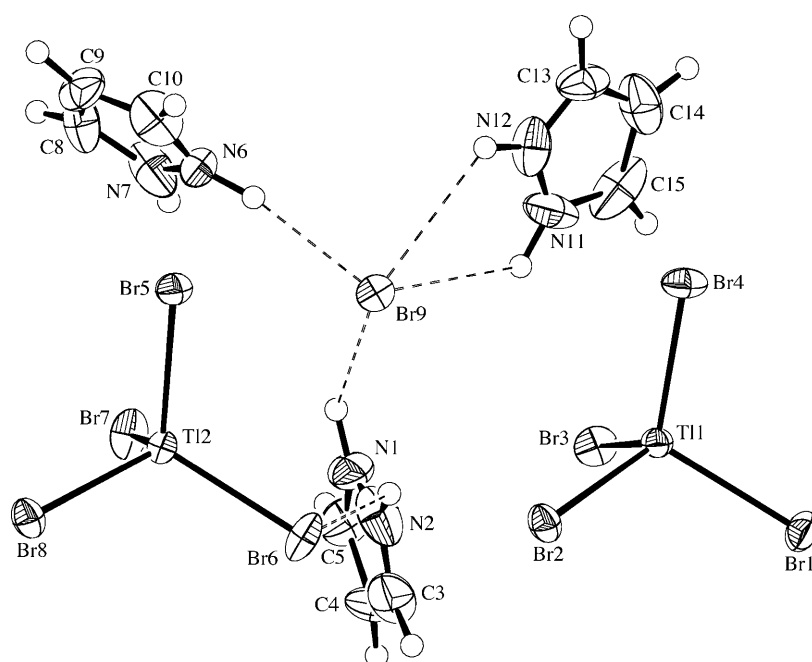Fig. 11. *The asymmetric unit in the structure of $[C_3H_5N_2]_3 \cdot [TlBr_4]_2 \cdot Br$ (5) showing the atom-labeling scheme and the pseudo-$[Tl_2B_9]^{3-}$ grouping.* Dashed lines represent H-bonds. The displacement ellipsoids are shown at the 50% probability level.

The Br^- ion in **5** accepts four $N-H\cdots Br$ H-bonds; one from each of two of the symmetry-independent cations and two from the third cation (*Table 9*). The former two cations also form H-bonds with two symmetry-related $[TlBr_4]^-$ anions (those

Table 8. *Selected Interatomic Distances* [Å] *and Angles* [°] *for* [$C_3H_5N_2$]$_3$ · [$TlBr_4$]$_2$ · Br (**5**), *with Standard Uncertainties in Parentheses*

Tl(1)–Br(1)	2.5506(7)	Tl(2) –Br(5)	2.5708(7)
Tl(1)–Br(2)	2.5442(7)	Tl(2)–Br(6)	2.5336(7)
Tl(1)–Br(3)	2.5716(8)	Tl(2)–Br(7)	2.5510(9)
Tl(1)–Br(4)	2.5306(7)	Tl(2)–Br(8)	2.5459(7)
Tl(1)···Br(9)	4.7923(8)	Tl(2)···Br(9)	4.4712(8)
Tl(1)···Tl(2)	7.6442(3)		
Br(1)–Tl(1)–Br(2)	109.52(2)	Br(5)–Tl(2)–Br(6)	113.08(3)
Br(1)–Tl(1)–Br(3)	105.37(3)	Br(5)–Tl(2)–Br(7)	108.46(3)
Br(1)–Tl(1)–Br(4)	111.33(2)	Br(5)–Tl(2)–Br(8)	105.65(2)
Br(2)–Tl(1)–Br(3)	107.07(3)	Br(6)–Tl(2)–Br(7)	107.83(2)
Br(2)–Tl(1)–Br(4)	113.08(2)	Br(6)–Tl(2)–Br(8)	112.96(3)
Br(3)–Tl(1)–Br(4)	110.11(3)	Br(7)–Tl(2)–Br(8)	108.72(3)
Br(1)–Tl(1)···Br(9)	173.55(2)	Br(5)–Tl(2)···Br(9)	69.65(2)
Br(2)–Tl(1)···Br(9)	71.00(2)	Br(6)–Tl(2)···Br(9)	73.90(2)
Br(3)–Tl(1)···Br(9)	68.64(2)	Br(7)–Tl(2)···Br(9)	68.98(2)
Br(4)–Tl(1)···Br(9)	73.71(2)	Br(8)–Tl(2)···Br(9)	173.05(2)
Tl(1)···Br(9)···Tl(2)	111.17(2)		

Table 9. *H-Bonding Parameters for* [$C_3H_5N_2$]$_3$ · [$TlBr_4$]$_2$ · Br (**5**), *with Standard Uncertainties in Parentheses*

D–H···A[a]	D–H [Å]	H···A [Å]	D···A [Å]	D–H···A [°]
N(1)–H(1)···Br(9)	0.88	2.66	3.285(7)	129
N(2)–H(2)···Br(6)	0.88	2.82	3.455(7)	130
N(6)–H(6)···Br(9)	0.88	2.41	3.281(7)	171
N(7)–H(7)···Br(5)[i]	0.88	2.52	3.365(7)	162
N(11)–H(11)···Br(9)	0.88	2.93	3.429(9)	118
N(12)–H(12)···Br(9)	0.88	2.79	3.368(7)	124

[a]) Symmetry operator: [i] $1/2 + x$, y, $3/2 - z$.

involving atom Tl(2)). These interactions serve to link the three cations, the Br$^-$ ion, and one of the two symmetry-independent [$TlBr_4$]$^-$ anions into continuous chains which run parallel to the [1 0 0] direction (*Fig. 12*). The sequence of H-bonded moieties through one repeat of this chain is ···Tl(2) ← cation B → Br$^-$ ← cation A → Tl(2′)···, while cation C is a side group which forms two H-bonds to the same Br$^-$ ion. The other symmetry-independent [$TlBr_4$]$^-$ anions (those involving atom Tl(1)) are not involved in any H-bonding interactions.

The atomic displacement parameters for the atoms of the three symmetry-independent cations in **5** are elongated in directions that are parallel to the plane of each five-membered ring. This observation suggests each of these rings may be disordered over two orientations related to each other by a pivot of the ring about an axis perpendicular to the ring plane. A similar disorder is often observed with cyclopentadienyl rings. Attempts to resolve this disorder into two orientations for each ring did not produce a satisfactory or stable model, even when a complex series of
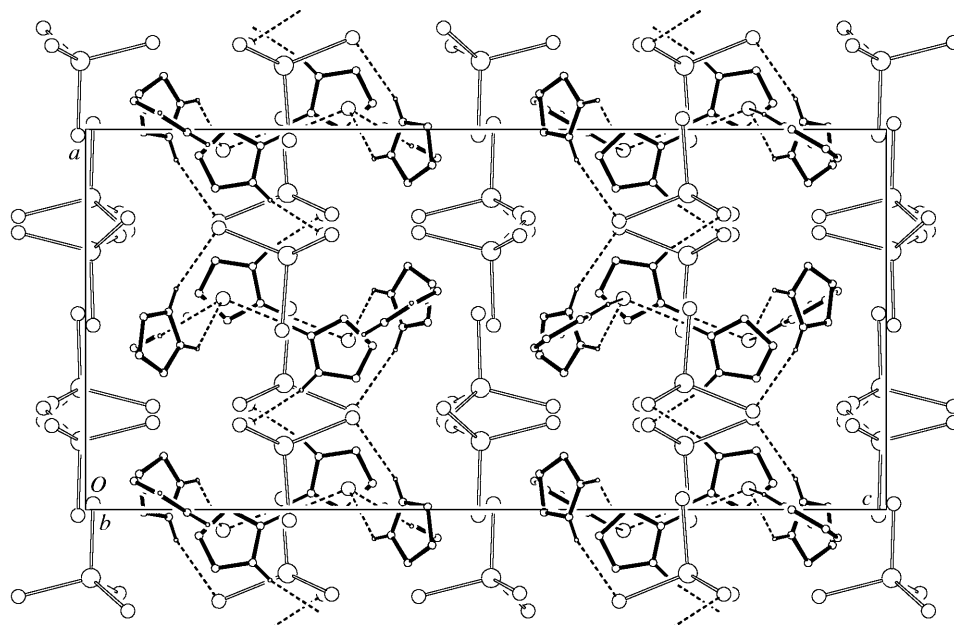
Fig. 12. *A projection of the crystal packing of **5** viewed down [0 1 0] showing the H-bonding as dashed lines.* The H-atoms bonded to C-atoms have been omitted for clarity.

similarity restraints was employed. As a consequence, the ordered model was employed for the final refinement, but the cation geometry should be taken as being only approximate due to the untreated disorder.

All of the other monovalent cations, **VI**–**XI** (*Table 1*), employed in this part of the study produced simple binary salts which contain tetrabromothallate(III) anions and have the [BaseH]·[TlBr$_4$] stoichiometry (compounds **6**–**11**; *Table 2*). These facts were confirmed by X-ray crystal-structure analyses for compounds **6**–**9**, as detailed below. For the piperidinium (**X**) and quinolinium (**XI**) salts **10** and **11**, crystal-structure determinations were not undertaken, but the *Raman* spectra showed Tl−Br stretching frequencies that are very similar to those observed for other compounds known from X-ray crystallography to possess tetrahedral [TlBr$_4$]$^-$ species [1][26], while the overall [TlBr$_4$]$^-$ stoichiometry was confirmed by the elemental analyses.

The anions in the crystal structure of 1,5-diazabicyclo[4.3.0]non-5-enium tetrabromothallate(III) (**6**) sit across mirror planes, while the cations lie over centers of inversion and are, therefore, disordered about the latter. The anion geometry is clearly defined and is a very regular tetrahedron (*Table 10*). The overlapping disordered orientations of the cations caused instability in the refinement of the atomic positions. Therefore, bond-length restraints were applied to most of the bonds within the cation in order to maintain reasonable geometry. Suitable values for the restraints were derived from the well-defined structure of (*S*)-9-(hydroxymethyl)-1,5-diazabicyclo[4.3.0]non-5-ene [33]. The positions of the H-atoms could not be located because of the disorder, and it is assumed that N(5) is protonated. This choice is based on the fact that the

Table 10. *Selected Interatomic Distances* [Å] *and Angles* [°] *for [C₇H₁₃N₂]·[TlBr₄]* (**6**)*, [C₉H₁₄N]·* *[TlBr₄]* (**7**)*, and [C₁₀H₁₀N₃]·[TlBr₄]* (**8**)*, with Standard Uncertainties in Parentheses*[a]

Complex **6**			
Tl−Br(1)	2.5518(8)	Tl−Br(3)	2.5528(5)
Tl−Br(2)	2.5559(8)		
Br(1)−Tl−Br(2)	110.31(3)	Br(2)−Tl−Br(3)	109.42(2)
Br(1)−Tl−Br(3)	108.15(2)	Br(3)−Tl−Br(3)ⁱ	111.38(3)
Complex **7**			
Tl−Br(1)	2.5562(5)	Tl−Br(3)	2.5697(6)
Tl−Br(2)	2.5326(7)	Tl−Br(4)	2.5418(7)
Br(1)−Tl−Br(2)	113.60(2)	Br(2)−Tl−Br(3)	110.11(2)
Br(1)−Tl−Br(3)	106.75(2)	Br(2)−Tl−Br(4)	109.40(4)
Br(1)−Tl−Br(4)	106.36(2)	Br(3)−Tl−Br(4)	110.53(3)
Complex **8**			
Tl−Br(1)	2.5675(4)	Tl−Br(3)	2.5693(4)
Tl−Br(2)	2.5459(4)	Tl−Br(4)	2.5524(4)
Br(1)−Tl−Br(2)	109.65(2)	Br(2)−Tl−Br(3)	107.66(2)
Br(1)−Tl−Br(3)	109.98(1)	Br(2)−Tl−Br(4)	115.33(2)
Br(1)−Tl−Br(4)	104.48(2)	Br(3)−Tl−Br(4)	109.69(2)

[a]) Symmetry operator: ⁱ $x, 3/2 − y, z$.

bridging bond, N(1)−C(6), is relatively short, *i.e.*, 1.32(1) Å, which suggests some delocalization of the electron density from the N(5)=C(6) bond (1.292(8) Å) to the N(1)−C(6) bond with the result that N(1) probably carries some of the positive charge. Furthermore, the sum of the angles around N(1) is 360°, so there is no evidence for any pyramidalization at this atom, which would occur if N(1) was protonated. Also, N(5) is closer to any Br-atom than N(1) and is, therefore, the most likely H-bond donor. The shortest N···Br distance is 3.79(2) Å for N(5)···Br(3), and the corresponding H···Br distance is 3.00 Å (*Table 11*). These distances are longer than the N−H···Br H-bonding distances normally found in the other bromothallate(III) complexes that have been studied and are probably at the margin of what might be considered an actual H-

Table 11. *H-Bonding Parameters for [C₇H₁₃N₂]·[TlBr₄]* (**6**) *and [C₁₀H₁₀N₃]·[TlBr₄]* (**8**)*, with Standard Uncertainties in Parentheses*

D−H···A[a])	D−H [Å]	H···A [Å]	D···A [Å]	D−H···A [°]
Complex **6**				
N(5)−H(5)···Br(3)	0.88	3.00	3.79(2)	150
Complex **8**				
N(3)−H(13)···Br(2)ⁱ	0.88	3.03	3.418(6)	109
N(3)−H(13)···Br(3)	0.88	2.67	3.526(6)	163
N(4)−H(14)···Br(1)ⁱⁱ	0.88	2.84	3.345(6)	118
N(4)−H(14)···Br(2)ⁱⁱⁱ	0.88	2.63	3.401(7)	148

[a]) Symmetry operators: ⁱ $1 − x, y − 1/2, 3/2 − z$; ⁱⁱ $1 − x, 1/2 + y, 3/2 − z$; ⁱⁱⁱ $1 − x, 1 − y, 1 − z$.

bonding interaction between the cation and the anion. The shortest $N(1) \cdots Br$ distance is 4.10(3) Å. As a result of the mirror symmetry of the anion, the $N(5)-H(5) \cdots Br(3)$ H-bond links two mirror-related cations and one anion into ion triplets (*Fig. 13*).
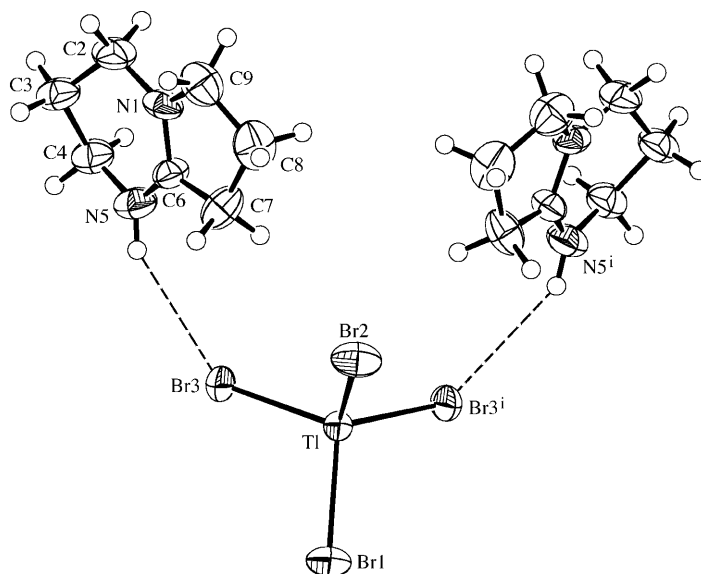

Fig. 13. *The structure of the H-bonded ion-triplet of [$C_7H_{13}N_2$] · [$TlBr_4$]* (**6**) *showing the atom-labeling scheme and 50% probability for the displacement ellipsoids.* The labels with superscripts indicate atoms generated from the unique atoms by mirror symmetry; the other inverted, superimposed orientation of the disordered cation has been omitted for clarity.

The determination of the crystal structure of the tetrabromothallate(III) salt **9** of the related 1,8-diazabicyclo[5.4.0]undec-7-enium cation (**IX**) proved troublesome because of severe irresolvable disorder within the two symmetry-independent cations which reside in the asymmetric unit alongside two [$TlBr_4$]⁻ anions. The inadequacy of the model makes it inadvisable to provide a full discussion of the structure, other than to comment that the anions in the structure have been found unequivocally to be simple [$TlBr_4$]⁻ species, which is in agreement with the *Raman* spectrum and the stoichiometry derived from the elemental analysis.

The trimethyl(phenyl)ammonium tetrabromothallate(III) salt (**7**) is the only example in this entire study involving a monovalent quaternized cation. In the solid state, the ions do not possess any crystallographic symmetry. The anion is a pure [$TlBr_4$]⁻ species with no short contacts to other Br-atoms, and the tetrahedron is virtually undistorted (*Table 10* and *Fig. 14*). Although quaternized cations have been found to be a requirement for the formation of true [$TlBr_5$]²⁻ anions [1][2][4][6], an additional requirement is that such cations must either be divalent or, if monovalent, in sufficient excess to provide the required charge balance. In the case of compound **7**, the use of a 1 : 1 cation/anion ratio has resulted in the [$TlBr_4$]⁻ salt, which indicates that, in the absence of excess cation, an equilibrium in favor of the formation of bis[trimethyl(phenyl)ammonium] pentabromothallate(III) does not exist.
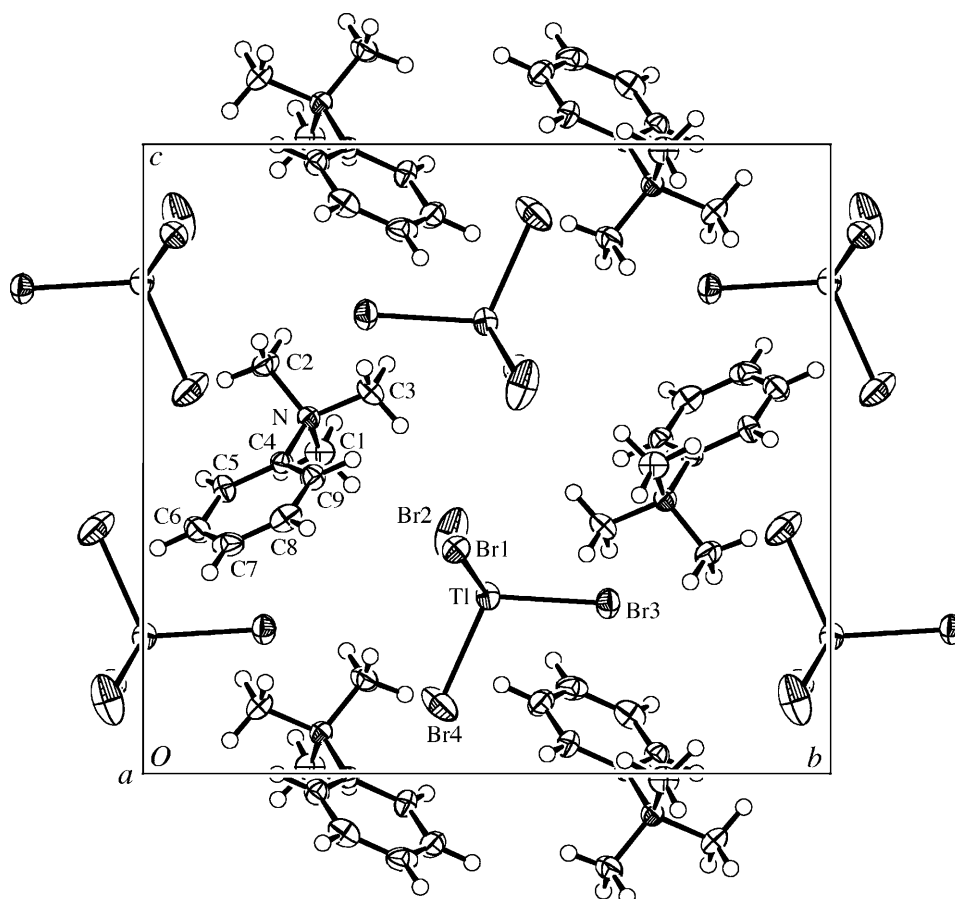
Fig. 14. *A projection of the crystal packing of [C₉H₁₄N]·[TlBr₄] (**7**) viewed down [100] showing the atom-labeling scheme and 50% probability for the displacement ellipsoids*

The anion in the crystal structure of (pyridin-2-yl)-(2-pyridinium)amine tetrabromothallate(III) (**8**) is a pure $[\text{TlBr}_4]^-$ species with no short contacts to other Br-atoms, and the tetrahedron is virtually undistorted (*Table 10*). There are two half-cations in the asymmetric unit, each of which is close to an inversion center. Expanding the cations about the inversion centers generates two full independent disordered cations, where the disorder superimposes inverted copies of the cations upon themselves (*Fig. 15*). This arrangement necessitated defining the amino N-atom in each cation with a site occupation factor of 0.5, while the site for each C-atom adjacent to the amino N-atom, as well as the sites of the pyridinyl and pyridinium N-atoms, are occupied by 0.5C + 0.5N. The arrangement of the cations in this structure is very similar to those in the $[\text{FeCl}_4]^-$ analogue [34] and in the (pyridin-2-yl)-(2-pyridinium)amine maleic acid (1/2) salt [35].

The positions of the H-atoms in **8** could not be located definitively because of the disorder. The cations could be protonated at the amino N-atom or at a pyridinyl N-
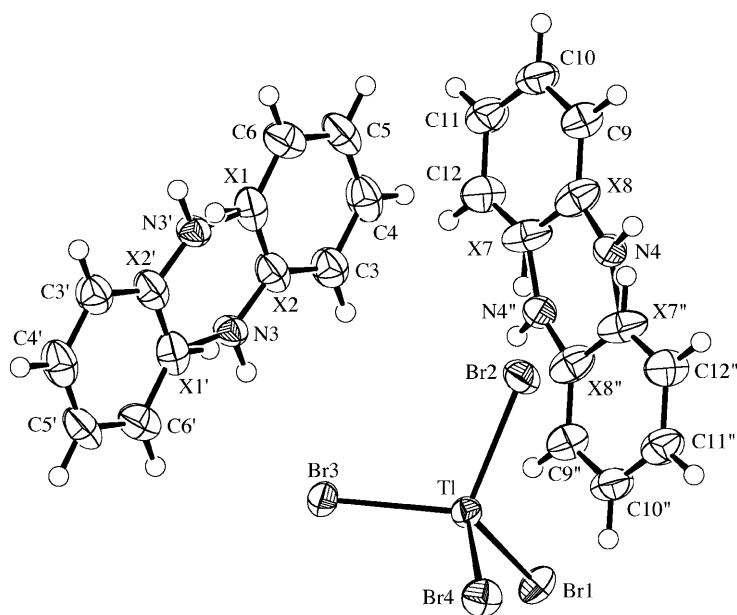
Fig. 15. *The components in the structure of [C₁₀H₁₀N₃]·[TlBr₄]* (**8**) *showing the atom-labeling scheme and 50% probability for the displacement ellipsoids.* The labels with ′ and ″ indicate atoms generated from the unique atoms by inversion centers. In the cations, N(3) and N(4) have occupancy 0.5, the sites denoted X(1), X(2), X(7), and X(8) are each occupied by 0.5C + 0.5N, and the H-atoms associated with N(3), N(4), X(1), and X(8) all have occupancy 0.5.

atom, or possibly even disordered between the two pyridinyl N-atoms. Protonation at any of these sites leads to a reasonable arrangement of H-bonds, so the presence or absence of H-bonds could not be used as a distinguishing tool in this case. However, while refinement of the various alternative models left the *R*-factor virtually unchanged, a test refinement of the isotropic atomic displacement parameters of the amino and pyridinium H-atoms led to reasonable values for these parameters only when the cations were defined as having one amino and one pyridinium H-atom, with the latter not being disordered between the two pyridinyl N-atoms. Also, the amino N–C bond lengths of *ca.* 1.35 Å are shorter than would be expected if the amino group was protonated.

The cations in **8** form bifurcated N–H···Br H-bonds to the Br-atoms of adjacent [TlBr₄]⁻ anions (*Table 11*). Ignoring the cation disorder, each of the symmetry-independent cations interacts with two [TlBr₄]⁻ anions, while each anion interacts with three cations, two of which are symmetry-related, and the third is the other symmetry-independent cation. The interaction between the anion and its two neighboring symmetry-related cations serves to link these ions into continuous chains, which run parallel to the crystallographic [0 1 0] direction (*Fig. 16*) and have a graph set motif [32] of $C_1^2(4)$. The other symmetry-independent cation connects the chains to a second anion, but the interactions are not propagated further, so that this cation–anion pair merely acts as a side group to the main chain. Propagation of the interionic H-bonds by
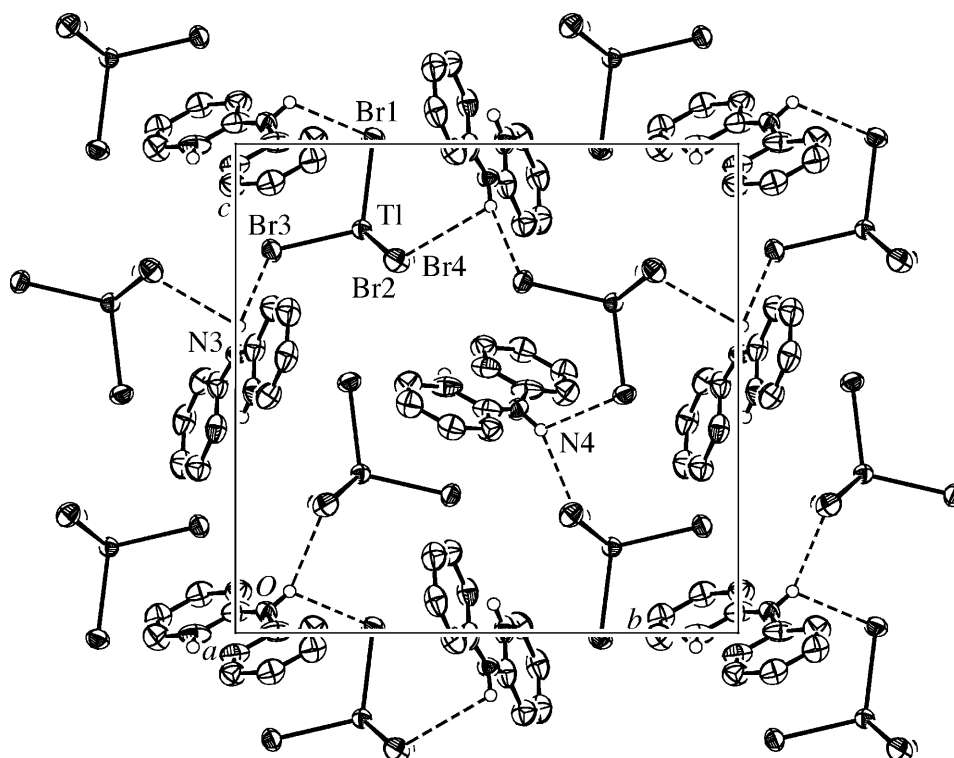
Fig. 16. *A projection of the crystal packing of* **8** *viewed down [1 0 0] showing the H-bonding as dashed lines and 50% probability for the displacement ellipsoids.* Only one orientation of each disordered cation is displayed. The H-atoms bonded to C-atoms have been omitted for clarity.

inversion of the cations leads to cooperative two-dimensional planar networks which lie perpendicular to the crystallographic [1 0 0] direction. The pyridinium N-atom is not close enough to any Br-atoms to indicate the presence of H-bonds between these atoms, but the usual intramolecular N−H···N interaction between the pyridinium and the pyridinyl N-atoms is present.

4. An Overview of the Structural Diversity and Predictability of Bromothallate(III) Anions. – In our extensive study of the structural diversity exhibited by bromothallate (III) anions, a total of 34 new organoammonium bromothallate(III) compounds were synthesized, and the crystal structures of 25 of these have been determined ([1][2][4 – 6] and this work). In the remaining cases, the nature of the anionic species present has been elucidated unambiguously on the basis of their *Raman* spectra and elemental analyses. The pertinent questions to which answers were sought in this project are:

- Do the anions in bromothallate(III) compounds show a rich structural diversity, or are the preferred anionic species limited to a few principal forms?
- Is it possible to generate new species with $[TlBr_5]^{2-}$ stoichiometry?
- Do discrete $[TlBr_5]^{2-}$ anions exist?

- If so, is their geometry square-pyramidal, or is a trigonal-bipyramidal coordination geometry preferred? One example of each geometry is known for discrete $[TlCl_5]^{2-}$ anions [36][37].
- Is there a preference for octahedral coordination of Tl^{III} by bromide, even in compounds without $[TlBr_6]^{3-}$ stoichiometry, as found with some chlorothallate(III) structures [38–44], which will lead to Br-bridged binuclear or polynuclear anions?
- What influence, if any, does $N-H\cdots Br$ H-bonding have on the anionic structures?
- What factors influence the metal ion complex groupings that are present?
- Can the structural groupings be rationalized, so that it is possible to predict them and/or design them?

The accumulated data now allow a detailed examination of trends and the factors influencing the nature of the anions that can be generated. This analysis forms the subject of the following discussion.

4.1. *The Structural Diversity of Bromothallate(III) Anions.* One of the principal aims of the project was to ascertain if the anions in bromothallate(III) salts exhibited a broad structural diversity, similar to the chlorothallate(III) salts, or if there was a preference for a more limited range of species, such as the already known $[TlBr_4]^-$ and $[TlBr_6]^{3-}$ anions. Since Tl^{III}, is a large d^{10} system, it could have the potential to exhibit a rich structural diversity similar to the huge diversity found for Hg^{II} complexes. Indeed, a diverse range of bromothallate(III) structures was found with eleven different types of anion, anion grouping, or mixed salt systems being observed. These eleven types are:

- $[BaseH]\cdot[TlBr_4]$
- $[Base^{2+}]\cdot[TlBr_5]$
- $[BaseH_3]\cdot[TlBr_6]$
- $[BaseH]_2\cdot[TlBr_4]\cdot Br$ or $[BaseH_2]\cdot[TlBr_4]\cdot Br$ with discrete anions
- $[BaseH_2]\cdot[TlBr_5]$ with one long axial $Tl\cdots Br$ secondary bond
- $[BaseH_2]\cdot[TlBr_5]$ with polymeric *cis*-bromo-bridged $[TlBr_5]^{2-}$ anions
- $[BaseH]_3\cdot[TlBr_4]_2\cdot Br$ arranged as a pseudo-$[Tl_2Br_9]^{3-}$ grouping
- $[BaseH_2]_4\cdot[TlBr_4]\cdot[TlBr_6]\cdot 4\,Br$
- $[Base^{2+}]_3\cdot[TlBr_4]_3\cdot[TlBr_6]$ with potential *cis*-bromo-bridged $[TlBr_4]_3^{3-}$ trimers
- $[BaseH_2]_2\cdot[TlBr_4]\cdot[TlBr_6]$
- $[BaseH_3]_2\cdot[TlBr_4]_3\cdot 3\,Br$

Despite this variety, the structural diversity is generally limited to various combinations of just four principal moieties, namely the $[TlBr_4]^-$, $[TlBr_5]^{2-}$, $[TlBr_6]^{3-}$, and Br^- anions. Even the pseudo-$[Tl_2Br_9]^{3-}$ groupings in the salts obtained from the pyrazolinium and pyridinium cations (**V** and **XVII**, resp.) are nothing more than conveniently arranged, but quite discrete combinations of $[TlBr_4]^-$ and Br^- ions. A degree of novel variation is observed among those salts containing $[TlBr_5]^{2-}$ anions with one long axial $Tl\cdots Br$ secondary bond where the $Tl\cdots Br$ distance covers a wide range of values (*vide infra* in *Sect. 4.5*, and also *Sect. 3.2*). One polynuclear structure was found, that being the *cis*-bromo-bridged $[TlBr_5]^{2-}$ anions of the N-methylpropane-1,3-diammonium (**XXVII**) salt, in which secondary $Tl\cdots Br$ bonds of 3.632(4) Å link the $[TlBr_5]^{2-}$ units [2]. A second structure might possibly be interpreted as having trinuclear anions. In the 1,1,3,3-tetramethylimidazolidinium (**XIII**) mixed salt, which

has the formulation $[Base^{2+}]_3 \cdot [TlBr_4]_3 \cdot [TlBr_6]$, the tetrahedral $[TlBr_4]^-$ anions are slightly distorted, and two very long *cis*-positioned secondary $Tl\cdots Br$ bonds of 3.975(2) Å from adjacent $[TlBr_4]^-$ ions complete an octahedral arrangement [4]. These interactions propagate about a crystallographic C_3 axis to give a *cis*-double-Br-bridged cyclic trinuclear $[Tl_3Br_{12}]^{3-}$ moiety. Despite the very long $Tl\cdots Br$ distances, the interactions must be significant, because noticeable distortion of the $[TlBr_4]^-$ tetrahedron occurs.

Thus, from the paucity of multinuclear anions found in the data accumulated so far, the bromothallate(III) anions do not appear to exhibit a structural diversity quite as rich as that found among the chlorothallate(III) salts, where binuclear species like $[Tl_2Cl_{10}]^{4-}$ [38][39], or extended chain structures, in which $[TlCl_5]^{2-}$ units are symmetrically or asymmetrically *cis*-Cl-bridged [39–43] or *trans*-Cl-bridged [44], have been observed more frequently.

The formation of binuclear or polynuclear $[TlCl_5]^{2-}$ species suggests that there might be a preference for the Tl-atom in chlorothallate(III) compounds to have octahedral coordination, even when the overall Tl/halogen stoichiometry is not 1:6. In contrast, the fact that only two polynuclear bromothallate(III) anionic structures were observed among the studied pentabromothallate(III) compounds, and then only as a result of quite weak secondary $Tl\cdots Br$ bonds, suggests that there is less of a preference for octahedral coordination at the Tl-atom in the case of bromothallate(III) salts, although octahedrally coordinated Tl^{III} was observed as discrete $[TlBr_6]^{3-}$ anions in four other compounds. Three of these involved the divalent cations **XIII**, **XIV**, and **XXVII** (see *Sect. 4.3*), so given the constantly used cation/TlBr$_3$ ratio of 1:1, the presence of $[TlBr_6]^{3-}$ as part of a mixed salt, instead of a $[TlBr_5]^{2-}$ anion or a $[TlBr_4]^-$/ Br$^-$ mixed salt, does suggest that octahedral Tl-coordination is favored under the right conditions. The fourth compound involved the trivalent cation **I** (see *Sect. 4.4*), which would be expected to favor the formation of a $[TlBr_6]^{3-}$ anion. Another similar trivalent cation, **II**, however, produced the $[BaseH_3]_2 \cdot [TlBr_4]_3 \cdot 3\,Br$ arrangement of compound **2**, which is completely free of octahedrally coordinated Tl-atoms. All of these results suggest that octahedral coordination at the Tl-atom only occurs when all other contributing factors like ion-size distribution and required charge balance are appropriate, rather than the drive to attain octahedral coordination being a dominating influence.

4.2. *Salts Obtained with Monovalent Cations.* Of the 34 organoammonium cations employed, 17 were monovalent, and these are depicted in *Table 12*. *Basolo*'s general principle [25] states: '*Solid salts separate from aqueous solution easiest for combinations of either small cation–small anion or large cation–large anion, preferably with systems having the same but opposite charges on the counterions*'. As all syntheses were restricted deliberately to the use of a cation/TlBr$_3$ ratio of 1:1, one might, therefore, expect the monovalent cations to yield bromothallate(III) salts with a corresponding monovalent anion of similar size, namely $[TlBr_4]^-$. Although the syntheses employed the bromide salt of the organic base, *Basolo*'s hypothesis suggests that the inherent size mismatch between the bulky cations and the Br$^-$ ion would not favor the reappearance of the simple bromide salt upon crystallization. Indeed, 13 of the employed monovalent cations yielded the straightforward $[BaseH] \cdot [TlBr_4]$ salts, as do the 2,5-dimethylpyrazinium and (2-phenylethyl)ammonium cations [45][46].

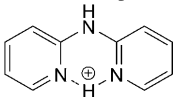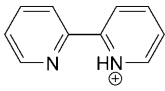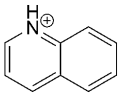Table 12. *Monovalent Cations Used to Generate Bromothallate(III) Salts and Where Described*
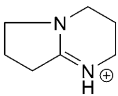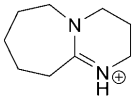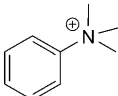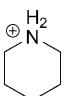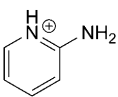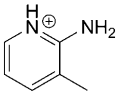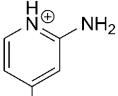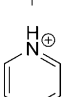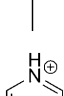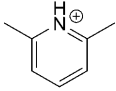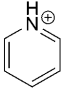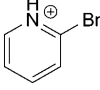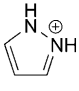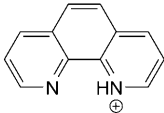
Cations that produced [TlBr₄]⁻ salts

	(Pyridin-2-yl)-(2-pyridinium)amine (**VIII**)	This work
	2-(Pyridin-2-yl)pyridinium (**XXXIV**)	[5]
	Quinolinium (**XI**)	This work
	1,5-Diazabicyclo[4.3.0]non-5-enium (**VI**)	This work
	1,8-Diazabicyclo[5.4.0]undec-7-enium (**IX**)	This work
	Trimethyl(phenyl)ammonium (**VII**)	This work
	Piperidinium (**X**)	This work
	2-Aminopyridinium (**XXVIII**)	[1]
	2-Amino-3-methylpyridinium (**XXIX**)	[1]
	2-Amino-4-methylpyridinium (**XXX**)	[1]
	4-Methylpyridinium (**XXXI**)	[1]
	4-(Dimethylamino)pyridinium (**XXXII**)	[1]

Table 12 (cont.)

	2,6-Dimethylpyridinium (**XXXIII**)	[1]

Cations that produced mixed salts

	Pyridinium (**XVII**)	[1]
	2-Bromopyridinium (**XVIII**)	[1]
	Pyrazolinium (**V**)	This work
	1,10-Phenanthrolinium (**XV**)	[5]

The four remaining monovalent cations, **V**, **XV**, **XVII**, and **XVIII**, produced mixed salt arrangements in which $[TlBr_4]^-$ and Br^- ions were present as essentially discrete entities [1], although it could be argued that there is some very weak $Tl \cdots Br$ secondary bonding in the 2-bromopyridinium (**XVIII**) and 1,10-phenanthrolinium (**XV**) salts to give $[TlBr_4]^- \cdots Br^-$ ion association in the former ($Tl \cdots Br = 4.1545(6)$ Å) and extended $[TlBr_4]^- \cdots [TlBr_4]^-$ chains in the latter ($Tl \cdots Br = 4.099(1)$ Å). The pyrazolinium and pyridinium salts from cations **V** and **XVII** have the general formula $[BaseH]_3 \cdot [TlBr_4]_2 \cdot Br$ and contain a pseudo-$[Tl_2Br_9]^{3-}$ grouping, which gives a cation/Tl/Br ratio of $3:2:9$, while those from **XV** and **XVIII** have the general formula $[BaseH]_2 \cdot [TlBr_4] \cdot Br$, giving a cation/Tl/Br ratio of $2:1:5$. Another question arises: why do these four outlier compounds form? The size of the cation may play a role here, although clearly there are too many variables to make definite assertions. The planar cations **V** and **XVII** are the smallest of all the monovalent cations employed. If these are now too small to match well with the size of the $[TlBr_4]^-$ anion and give the usual $[BaseH] \cdot [TlBr_4]$ salt, it may be possible to rectify the mismatch if the total volume occupied by the anions is shrunk slightly, which could be achieved by periodically doping the anionic lattice of $[TlBr_4]^-$ anions with something smaller. Replacing every third $[TlBr_4]^-$ anion with Br^- would be one way to achieve a reduced volume and essentially results in the structures observed in these compounds. The piperidinium cation (**X**) might be thought to have a small size similar to that of the pyridinium ion, but the former is nonplanar, and the additional H-atoms provide increased bulkiness, so it is probably not surprising that the usual $[TlBr_4]^-$ salt resulted.

A similar size-based argument could be applied to the 1,10-phenanthrolinium (**XV**) and 2-bromopyridinium (**XVIII**) salts, where it might be imagined that every second

$[TlBr_4]^-$ anion has been replaced by Br^-. However, such a pattern would only be logical if these cations were even smaller than the pyridinium and pyrazolinium cations, which is not the case. Cation **XV** is among the largest employed, although it is two-dimensional because of its planarity, while the size of cation **XVIII** is barely different from those of the 2-aminopyridinium cation (**XXVIII**) and the related substituted pyridinium cations **XXIX – XXXIII**, all of which produced $[BaseH] \cdot [TlBr_4]$ compounds, although the Br substituent would introduce a unique polarity into **XVIII**. Thus, cation size is not necessarily the only influence dominating the nature of the bromothallate(III) salts of the monovalent cations. The number of $N-H$ H-bond donors available on the cations probably also has little influence, as simple $[TlBr_4]^-$ salts are obtained with cations having anything from zero to three donors, while different anionic structures are obtained among those cations having just one donor.

The predictability of the anionic bromothallate(III) species obtained in the presence of monovalent organoammonium cations is only moderate. While simple $[TlBr_4]^-$ salts are produced in the majority of cases, and $[TlBr_4]^-$ anions appear in every compound, the likelihood of the production of mixed salts cannot be excluded, although all of the mixed salts contain just additional amounts of Br^- ions. So far, no other bromothallate(III) species has been observed in conjunction with a monovalent cation, provided the tentative very weak $[TlBr_4]^- \cdots Br^-$ secondary bonding suggested for the 2-bromopyridinium salt [1] is considered to be insignificant.

4.3. *Salts Obtained with Divalent Cations.* A total of 15 divalent organoammonium cations were used in the study, and these are depicted in *Table 13*. It was anticipated that these bulky divalent anions would stabilize the corresponding divalent $[TlBr_5]^{2-}$ anion, which had not been observed definitively prior to this project, or at least generate a salt with the $[TlBr_5]^{2-}$ stoichiometry. A true discrete $[TlBr_5]^{2-}$ anion with quite regular coordination geometry proved to be quite elusive, being obtained with only three cations, **XXIV – XXVI**, all of which were quaternized and, therefore, could not act as H-bond donors. More frequently, it was found that the compound contained either discrete $[TlBr_4]^-$ and Br^- ions (three compounds, from cations **XVI**, **XIX**, and **XX**), or that weak secondary bonding between $[TlBr_4]^-$ and Br^- ions was present, thereby giving a $[TlBr_4]^- \cdots Br^-$ formulation in which the $Tl \cdots Br$ distance was found to range between 3.40 and 4.02 Å (five compounds, from cations **III**, **IV**, and **XXI – XXIII**). The 1-benzylpiperazinium compound **4** in this latter category has the longest $Tl \cdots Br$ distance, and it is difficult to decide if it should be referred to as a salt with discrete or partially associated Br^- ions. All of the above compounds at least have the anticipated $[TlBr_5]^{2-}$ stoichiometry. The *N*-methylpropane-1,3-diammonium cation (**XXVII**) produced a polymeric anionic species [2]. While this also had $[TlBr_5]^{2-}$ stoichiometry, the sixth coordination site in an otherwise square-pyramidal $[TlBr_5]^{2-}$ anion is occupied by a secondary $Tl \cdots Br$ bond of 3.632(4) Å to the Br-atom of a neighboring $[TlBr_5]^{2-}$ entity, thereby generating *cis*-Br-bridged chains of $[TlBr_5]^{2-}$ units.

The final three compounds are mixed salts, only one of which has $[TlBr_5]^{2-}$ stoichiometry: the *N,N*-diethylpropane-1,3-diammonium (**XII**) salt with the formulation $[BaseH_2]_2 \cdot [TlBr_4] \cdot [TlBr_6]$. Cation **XIV** yielded a mixed salt of the formulation $[BaseH_2]_4 \cdot [TlBr_4] \cdot [TlBr_6] \cdot 4 Br$ with the $[TlBr_7]^{4-}$ stoichiometry [2], while cation **XIII** produced a mixed salt of the formulation $[Base^{2+}]_3 \cdot [TlBr_4]_3 \cdot [TlBr_6]$, which gives

a cation/Tl/Br ratio of 3:4:18 [4]. This compound can also be described using the $[Base^{2+}]_3 \cdot [Tl_3Br_{12}] \cdot [TlBr_6]$ formulation if very weak secondary $Tl \cdots Br$ bonding between the $[TlBr_4]^-$ anions is taken into consideration.

Other than the influence of the quaternized cations on the formation of discrete $[TlBr_5]^{2-}$ anions, as *Table 13* shows, there appears to be little correlation between the size, shape, bulk or charge of the cations, and the nature of the anionic species they stabilize.

4.4. *Salts Obtained with Trivalent Cations*. Only two trivalent cations were employed, as depicted in *Table 14* and described in *Sect. 3.1*. Despite their similarities, the anionic species that they generated are quite different. The diethylenetriammonium cation gave a straightforward $[BaseH_3] \cdot [TlBr_6]$ salt (**1**), in line with *Basolo*'s principle, but the *N,N,N',N'',N''*-pentamethyldiethylenetriammonium cation produced a mixed salt with the formulation $[BaseH_3]_2 \cdot [TlBr_4]_3 \cdot 3\,Br$ (**2**), which gives a cation/Tl/ Br ratio of 2:3:15. As discussed above, it is assumed that the larger cation is less compatible with the size of the $[TlBr_6]^{3-}$ anion, so the anionic arrangement expands into one that requires more volume, but still maintains the required charge balance.

4.5. *The Formation and Structure of [TlBr₅]²⁻ Anions*. One objective of this project was to determine if the discrete $[TlBr_5]^{2-}$ anion could be generated, and, if so, whether it would adopt a trigonal-bipyramidal or square-pyramidal coordination geometry. Only two unambiguous solid-state structures involving a discrete $[TlCl_5]^{2-}$ ion are known and provide one example of each of these geometries [36][37], so afford no indication of a preferred coordination geometry for pentahalothallate(III) anions. The initial investigations utilized the piperazinium and 2,2'-bipyridinium cations (**XXI** and **XXII**, resp.), which produced two examples of an incipient $[TlBr_5]^{2-}$ species [5] with a highly distorted trigonal-bipyramidal coordination geometry about the Tl-atom, where one of the axial Tl−Br bonds was very long (*ca.* 3.77 Å). This long bond can be described as a secondary bond between a $[TlBr_4]^-$ moiety and a Br^- ion [30][31]. Further efforts then led to three salts with much more regular trigonal-bipyramidal $[TlBr_5]^{2-}$ anions (*Table 13*) [2][4][6]. Of these, the salt of the 1,1,4,4-tetramethylpiperazinium cation (**XXVI**) was found to have two polymorphs. The only compound that appeared to contain square pyramidal $[TlBr_5]^{2-}$ anions was that from the *N*-methylpropane-1,3-diammonium cation (**XXVII**) but, in this case, the Tl-atom actually has distorted octahedral coordination with one long secondary $Tl \cdots Br$ bond of 3.632(4) Å bridging adjacent $[TlBr_5]^{2-}$ moieties into polymeric anions.

The least distorted-trigonal bipyramidal $[TlBr_5]^{2-}$ anions were observed in the second polymorph involving cation **XXVI** [6] and the salt from cation **XXIV** [2]. In each of these structures, the axial Tl−Br bond lengths are equal, because each anion has crystallographic C_2 symmetry, although the axial Br−Tl−Br angle is distorted slightly from 180°. At 2.7350(5) and 2.762(2) Å in the salts from cations **XXVI** and **XXIV**, respectively, these Tl−Br bonds are the shortest of the longer of the two axial Tl−Br bonds found in any of the structures containing $[TlBr_5]^{2-}$ species. This feature is only logical, as any axial distortions will only serve to elongate one of the axial Tl−Br bonds. These distances could be deemed to represent the lengths of standard single Tl−Br bonds in the axial positions of a trigonal-bipyramidal environment. They are *ca.* 0.14 Å longer than the equatorial Tl−Br bonds, a trend which is generally the case in trigonal-bipyramidal complexes because of the *trans*-effect.

Table 13. *Divalent Cations Used to Generate Bromothallate(III) Salts and Where Described*
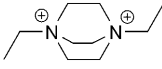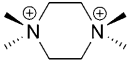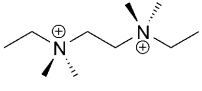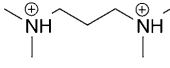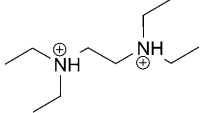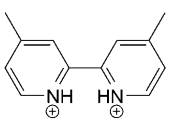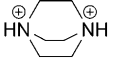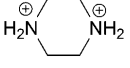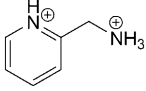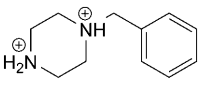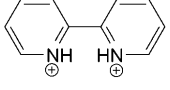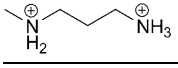
Cations resulting in regular [TlBr₅]²⁻ anions

    N,N′-Diethyltriethylenediammonium (**XXV**)   [4]

    1,1,4,4-Tetramethylpiperazinium (**XXVI**) (two polymorphs)   [4][6]

    N,N′-Diethyl-N,N,N′,N′-tetramethylethylene-1,2-diammonium (**XXIV**)   [2]

Cations resulting in discrete [TlBr₄]⁻ and Br⁻ ions

    N,N,N′,N′-Tetramethylpropane-1,3-diammonium (**XIX**)   [2]

    N,N,N′,N′-Tetraethylethylene-1,2-diammonium (**XX**)   [2]

    4,4′-Dimethyl-2,2′-bipyridinium (**XVI**)   [5]

Cations resulting in secondary [TlBr₄]···Br bonds

    Triethylenediammonium (**III**)   This work

    Piperazinium (**XXI**)   [5]

    2-(Ammoniomethyl)pyridinium (**XXIII**)   [1]

    1-Benzylpiperazinium (**IV**)   This work

    2,2′-Bipyridinium (**XXII**)   [5]

Cation resulting in bromo-bridged chains of [TlBr₅]²⁻ units

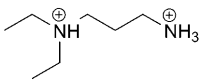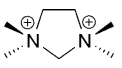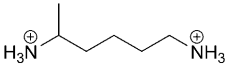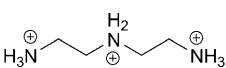   N-Methylpropane-1,3-diammonium (**XXVII**)   [2]

Table 13 (cont.)
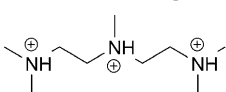
Cations that produced mixed salts		
	N,N-Diethylpropane-1,3-diammonium (**XII**)	[2]
	1,1,3,3-Tetramethylimidazolidinium (**XIII**)	[4]
	Hexane-1,5-diammonium (**XIV**)	[2]

Table 14. *Trivalent Cations Used to Generate Bromothallate(III) Salts and Where Described*

Produced a [TlBr$_6$]$^{3-}$ anion		
	Diethylenetriammonium (**I**)	This work
Produced discrete [TlBr$_4$]$^-$ and Br$^-$ ions		
	N,N,N′,N″,N″-Pentamethyldiethylenetriammonium (**II**)	This work

The first polymorph of the 1,1,4,4-tetramethylpiperazinium salt also had a reasonably regular trigonal-bipyramidal [TlBr$_5$]$^{2-}$ anion, but without the ion possessing any crystallographic symmetry [4]. The geometry of this [TlBr$_5$]$^{2-}$ anion is slightly more distorted than those possessing crystallographic symmetry, with one of the axial Tl−Br bonds being, at 2.840(1) Å, a little longer than in the symmetrical anions. The [TlBr$_5$]$^{2-}$ anion in the diethyl-DABCO (**XXV**) salt is distorted a little further with one of the axial Tl−Br bond lengths being 2.914(4) Å [4].

Other divalent cations led to more examples of the highly distorted [TlBr$_5$]$^{2-}$ species in which secondary Tl⋯Br bonds are present, and even to salts with just discrete [TlBr$_4$]$^-$ and Br$^-$ ions. The various categories are listed in *Table 13*. The remarkable observation is that the trigonal-bipyramidal [TlBr$_5$]$^{2-}$ moieties are not restricted to a limited number of forms, such as a regular form with little distortion and a distorted form in which the degree of distortion or length of the axial secondary Tl⋯Br bond is essentially constant. Instead, there is almost a continuum between the undistorted form at one extreme and completely discrete [TlBr$_5$]$^{2-}$ and Br$^-$ ions at the other, passing along the way through various levels of increasing [TlBr$_4$]⋯Br distortion by elongation of one of the axial Tl−Br bonds. These variations are listed in *Table 15*.

Fig. 17 shows the plot of the longest axial Tl−Br or Tl⋯Br distance *vs.* the mean of the angles between the shorter axial Tl−Br bond, and the equatorial Tl−Br bonds in [TlBr$_5$]$^{2-}$ and pseudo-[TlBr$_5$]$^{2-}$ species. This angle should be 90° for an undistorted trigonal-bipyramidal [TlBr$_5$]$^{2-}$ anion and 109.5° for a tetrahedral [TlBr$_4$]$^-$ anion. The

Table 15. *The Longest Tl···Br Distances in [TlBr$_5$]$^{2-}$ and Pseudo-[TlBr$_5$]$^{2-}$ Species*

Reference	Cation	Tl···Br [Å]
[6]	1,1,4,4-Tetramethylpiperazinium (**XXVI**, polymorph 2)	2.7350(4)
[2]	*N,N′*-Diethyl-*N,N,N′,N′*-tetramethylethylene-1,2-diammonium (**XXIV**)	2.762(2)
[4]	1,1,4,4-Tetramethylpiperazinium (**XXVI**, polymorph 1)	2.840(1)
[4]	*N,N′*-Diethyltriethylenediammonium (diethyl-DABCO, **XXV**)	2.914(4)
[1]	2-(Ammoniomethyl)pyridinium (**XXIII**)	3.400(2)
This work	Triethylenediammonium (DABCO, **III**)	3.6252(5)
[5]	Piperazinium (**XXI**)	3.769(2)
[5]	2,2′-Bipyridinium (**XXII**)	3.775(1)
This work	1-Benzylpiperazinium (**IV**)	4.0224(4)
[1]	2-Bromopyridinium (**XVIII**)	4.1545(6)
[1]	Pyridinium (**XVII**, pseudo-[Tl$_2$Br$_9$]$^{3-}$ with discrete [TlBr$_4$]$^-$ and Br$^-$)	4.5204(9), 4.6370(8)
This work	Pyrazolinium (**V**, pseudo-[Tl$_2$Br$_9$]$^{3-}$)	4.4712(8), 4.7923(8)

plot demonstrates the wide range of Tl···Br distances observed for the gradual inclusion of a fifth Tl···Br interaction in a core [TlBr$_4$]$^-$ unit. The line of best fit has been calculated for all structures in which the Tl···Br distance is less than 4.2 Å, and shows a good linear fit of the data. If one extrapolates the line to an angle of 109.5°, at which point there should be no significant distortion-causing interaction between the [TlBr$_4$]$^-$ and Br$^-$ ions, the corresponding Tl···Br distance is 4.35 Å, which fits remarkably well with that for the sum of the *Van der Waals* radii of the Tl- and Br-atoms [29]. Four additional points with Tl···Br distances greater than 4.2 Å, which are taken from the two structures with pseudo-[Tl$_2$Br$_9$]$^{3-}$ groupings (compound **5** and the pyridinium salt [1]), have been included in the plot. These represent examples in which there is no significant interaction between the [TlBr$_4$]$^-$ and Br$^-$ ions, and thus demonstrate the scatter of small distortions found in crystal structures of compounds containing normal tetrahedral [TlBr$_4$]$^-$ anions.
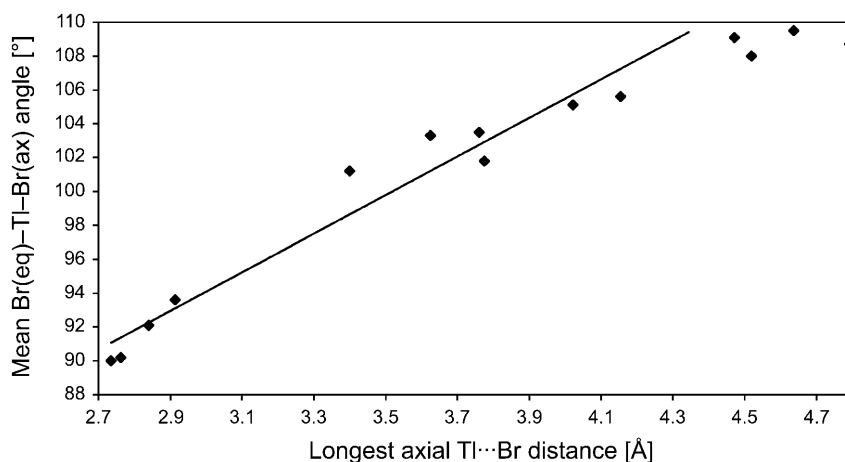

Fig. 17. *The trend between the longest axial Tl–Br distance, and the mean of the angles between the shorter axial Tl–Br bond and the equatorial Tl–Br bonds in [TlBr$_5$]$^{2-}$ and pseudo-[TlBr$_5$]$^{2-}$ species*

A second plot, shown in *Fig. 18*, indicates the trend between the longest axial Tl$\cdots$Br distance, and the mean of the lengths of the equatorial Tl−Br bonds in the [TlBr$_5$]$^{2-}$ and pseudo-[TlBr$_5$]$^{2-}$ species. The error bars on the graph have been set at 0.006 Å, which is an approximation to three times the standard uncertainties of the Tl−Br distances in most of the structures (actual range 0.0012 – 0.012 Å), and, therefore, gives an indication of the significance of the variations. Thus, the points to the right of *ca.* 3.6 Å on the abscissa can be considered to be a scatter about the horizontal line expected when ideal tetrahedral [TlBr$_4$]$^-$ geometry is reached, rather than representing a slight hump after a minimum. As would be expected, the equatorial Tl−Br bonds become shorter as the axial Tl$\cdots$Br distance increases, because the withdrawal of one Br$^-$ ion from the [TlBr$_5$]$^{2-}$ moiety reduces the electron density on the Tl-atom, which allows the remaining Br-atoms to move closer to the metal in compensation. However, the decrease stops when the Tl$\cdots$Br distance reaches *ca.* 3.6 Å, which is well short of the 4.35 Å limit given above for geometric distortion effects. This feature suggests that, although the fifth Br$^-$ ion causes significant distortion of the [TlBr$_4$]$^-$ tetrahedron when it approaches to a distance less than the sum of the *Van der Waals* radii of the Tl- and Br-atoms, there is negligible net donation of electron density from this Br$^-$ ion to the Tl-atom *via* coordination bonding until the distance becomes shorter than *ca.* 3.6 Å. This evidence might be used to argue that there is no secondary bonding interaction at a Tl$\cdots$Br distance beyond 3.6 Å, but if that is the case, why do some structures exist with longer Tl$\cdots$Br distances that are still significantly less than the sum of the *Van der Waals* radii of the Tl- and Br-atoms? In the absence of an electronic interaction, steric repulsion would be expected to prevent the Br$^-$ ion from approaching the [TlBr$_4$]$^-$ anion closer than the limiting *Van der Waals* distance. Either the [TlBr$_4$]$^-$ anion is sufficiently flexible to allow another Br$^-$ ion to come quite close without significant repulsive forces developing between the ions, when such a close approach is energetically optimal for efficient crystal packing, or there are indeed weak attractive forces between the [TlBr$_4$]$^-$ and Br$^-$ ions, which result from some orbital interactions and, therefore, the beginnings of bonding between the species, without this bonding
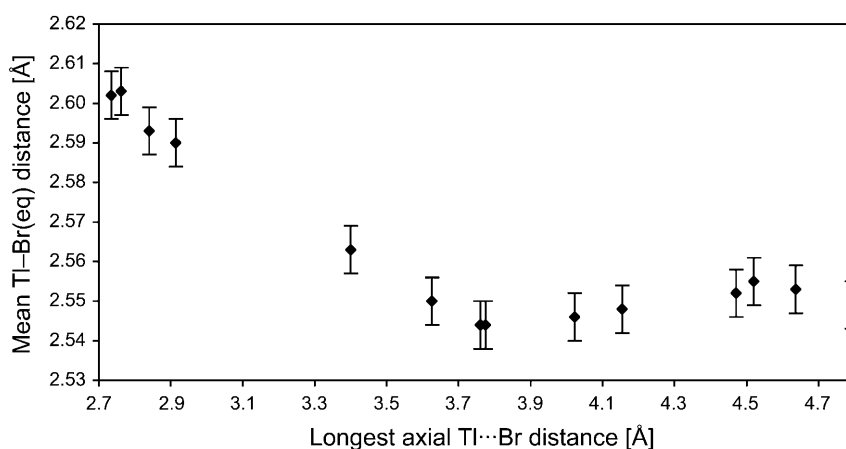

Fig. 18. *The trend between the longest axial Tl−Br distance, and the mean of the lengths of the equatorial Tl−Br bonds in [TlBr$_5$]$^{2-}$ and pseudo-[TlBr$_5$]$^{2-}$ species*

being sufficiently strong to cause discernable elongation of those Tl−Br bonds that would become equatorial in a formal $[TlBr_5]^{2-}$ anion.

Support for the latter concept of orbital interactions may be found in the theory of secondary bonding [30][31] where it was suggested that d orbitals on the central atom may mix with the bonding or non-bonding three-center orbitals involving the linear Y−A···X disposed atoms, these being the axially arranged Br−Tl···Br atoms in the distorted $[TlBr_5]^{2-}$ anions. It is conceivable that when the secondary bond is very weak, the donation of electron density to the Tl-atom *via* the dative coordination bond is balanced by back-donation through the metal d orbitals, so that there is no net accumulation of electron density on the Tl-atom and, therefore, no elongation of the equatorial Tl−Br bonds from the lengths they display in $[TlBr_4]^-$ anions. However, when the secondary Tl···Br bond is shorter than *ca.* 3.6 Å, the greater extent of σ-orbital overlap dominates the back-bonding effect and results in an increase of electron density on the Tl-atom. As a result, the equatorial Tl−Br bonds become noticeably longer, as exemplified in *Fig. 18*. The effect of the presence of N−H···Br H-bonding on the formation of $[TlBr_5]^{2-}$ ions, which will be discussed below, may also provide a hint that a weak bonding effect is present.

As hypothesized previously, an analysis of all the data now available shows one pattern that has clearly developed among the pentabromothallate(III) structures: secondary Tl···Br bonding occurs to give a highly distorted $[TlBr_5]^{2-}$ anion when the anion is involved in N−H···Br H-bonding with the cation. In all cases, the H-bonding interactions occur predominantly, if not exclusively, with the Br-atom that is most distant from the Tl-atom. These very long Tl···Br distances, or even structures with essentially discrete $[TlBr_4]^-$ and Br^- ions, manifest themselves consistently in the presence of cations with N−H H-bond donors, whereas the much more regular $[TlBr_5]^{2-}$ anions are obtained only in the presence of quaternary organoammonium cations, which, by their nature, preclude H-bonding. These observations suggest that the N−H···Br H-bonding is interfering with the ability of the fifth Br-atom to form a normal single bond with the Tl-atom by withdrawing electron density from the corresponding Tl−Br bond and thereby weakening the bond.

This study has included two pairs of compounds having cations with the same structural core and charge, but one cation in each pair has N−H H-bond donors, whereas the other cation does not, because it is quaternized. One of these pairs involves the triethylenediammonium (DABCO, **III**) and diethyl-DABCO (**XXV**) cations, while the other pair consists of the piperazinium (**XXI**) and 1,1,4,4-tetramethylpiperazinium (**XXVI**) cations. The quaternized cations **XXV** and **XXVI** produce bromothallate(III) salts with reasonably undistorted trigonal-bipyramidal $[TlBr_5]^{2-}$ anions, whereas cations **III** and **XXI** yield compounds containing highly distorted $[TlBr_5]^{2-}$ anions, in which secondary Tl···Br bonding results in the stretched $[TlBr_4]···Br$ extreme. The consistent behavior within the pairs seems to provide quite hard evidence that it is the presence or absence of the possibility for N−H···Br H-bond formation which controls whether a normal or highly distorted $[TlBr_5]^{2-}$ species is obtained. However, the use of a divalent quaternized organoammonium cation does not guarantee the formation of a salt with a regular $[TlBr_5]^{2-}$ anion, because the 1,1,3,3-tetramethylimidazolidinium cation (**XIII**) has been found to crystallize in a mixed salt containing $[TlBr_4]^-$ and $[TlBr_6]^{3-}$ anions, but not with $[TlBr_5]^{2-}$ [4].

The argument that the sizes of the cations play a role in the nature of the obtained $[TlBr_5]^{2-}$ species is weak. Admittedly, the spatial requirements for the cores of cations **III** and **XXVI** are not that different, as DABCO can be derived from piperazine simply by the addition of a third ethylene group bridging the N-atoms, so the behavior of the quaternized and unquaternized DABCO and piperazinium pairs might fortuitously be similar. Nevertheless, although the quaternized cation in each of these pairs is larger than its counterpart, because of the additional Et or Me groups, the cation size is probably not the factor influencing the geometry of the $[TlBr_5]^{2-}$ anions. Many of the other investigated salts of divalent cations, in which highly distorted $[TlBr_5]^{2-}$ anions, or even essentially discrete $[TlBr_4]^-$ and Br^- ions, were found, also have cations that are larger and bulkier than cations **III** or **XXVI**. Such examples involving divalent ring-based cations are compound **4**, and the salts from cations **XVI**, **XXII**, and **XXIII**.

4.6. *Secondary Tl⋯Br Bonds in Bromothallate(III) Anions.* Examples of secondary bonding were found frequently among the salts containing trigonal-bipyramidal $[TlBr_5]^{2-}$ anions, as discussed in the previous section, although secondary bonding was also observed in a few additional compounds.

The *N*-methylpropane-1,3-diammonium cation (**XXVII**) produced a salt with $[BaseH_2] \cdot [TlBr_5]$ stoichiometry, but the Tl-atom has distorted octahedral coordination where the sixth coordination site in an otherwise square-pyramidal $[TlBr_5]^{2-}$ anion is occupied by a secondary Tl⋯Br bond of 3.632(4) Å to the Br-atom of a neighboring $[TlBr_5]^{2-}$ entity, thereby generating *cis*-Br-bridged chains of $[TlBr_5]^{2-}$ units [2].

The 1,10-phenanthrolinium (**XV**) salt, while having the general formula $[BaseH]_2 \cdot [TlBr_4] \cdot Br$, did not display secondary Tl⋯Br bonding between the $[TlBr_4]^-$ and Br^- ions. Instead, a very weak secondary Tl⋯Br bond occurs between $[TlBr_4]^-$ units to give extended $[TlBr_4] \cdots [TlBr_4]$ chains (Tl⋯Br 4.099(1) Å) [5].

In the mixed salt from the 1,1,3,3-tetramethylimidazolidinium cation (**XIII**), which has the formulation $[BaseH_2]_3 \cdot [TlBr_4]_3 \cdot [TlBr_6]$, the tetrahedral $[TlBr_4]^-$ anions are slightly distorted and two very long *cis*-positioned secondary Tl⋯Br bonds of 3.975(2) Å from adjacent $[TlBr_4]^-$ ions complete an octahedral arrangement. These interactions propagate about a crystallographic C_3 axis to give a *cis*-double-Br-bridged cyclic trinuclear $[Tl_3Br_{12}]^{3-}$ moiety. This structure is somewhat of an outlier, because the compound contains a quaternary organoammonium cation, so N−H⋯Br H-bonding is not in play here.

In compound **2**, which has the formulation $[BaseH_3]_2 \cdot [TlBr_4]_3 \cdot 3\, Br$, the shortest interionic Tl⋯Br distance of 4.2104(7) Å is between two symmetry-independent $[TlBr_4]^-$ anions and is just inside the value (*ca.* 4.3 Å) for the sum of the *Van der Waals* radii of the Tl- and Br-atoms. A slight distortion of the tetrahedral geometry of the acceptor $[TlBr_4]^-$ anions is observed, which is consistent with a small influence of the distant Br-atom on the geometry of this anion. If this interaction is taken as significant, the two anions involved could be described as a $[Tl_2Br_8]^{2-}$ unit, where a secondary Tl⋯Br bond bridges the two $[TlBr_4]^-$ moieties. The overall structure would then have the formulation $[C_9H_{26}N_3]_2 \cdot [Tl_2Br_8] \cdot [TlBr_4] \cdot 3\, Br$. However, given that the Tl−Br⋯Tl angle is quite sharp at 124°, instead of the much more linear Br-bridge found in the other cases, and the proximity of the Tl⋯Br distance to the *Van der Waals* limit, it is doubtful that this arrangement of the $[TlBr_4]^-$ anions represents the presence of true interactions in the form of Tl⋯Br secondary bonding.

These examples demonstrate that secondary bonding in bromothallate(III) salts is not restricted to interactions between $[TlBr_4]^-$ anions and lone Br^- ions, but may also involve adjacent bromothallate(III) complex anions.

The extensive range of axial distortion found in the $[TlBr_5]^{2-}$ anions, as shown in *Table 15*, raises the question as to where the line is drawn between an elongated normal $Tl-Br$ single bond and secondary $Tl \cdots Br$ bonding. It can be assumed that the axial $Tl-Br$ single bond, which is *ca.* 2.74 Å in the most symmetrical case, can withstand some elongation due to asymmetrisation of the coordination environment of the Tl-atom, while still retaining its normal single-bond character. In this regard, it seems reasonable to allow a $Tl-Br$ bond elongation tolerance of up to 0.2 Å, which would then encompass the top four entries in *Table 15* and enable these compounds to be classified as having discrete $[TlBr_5]^{2-}$ anions with normal bonding. The next entry in the table has a substantially longer axial $Tl \cdots Br$ distance with the jump being *ca.* 0.5 Å. While this gap in observed axial $Tl \cdots Br$ distances does not prove that there are not any, as yet undiscovered, complexes in which the longest axial $Tl-Br$ distance is somewhere between 2.9 and 3.4 Å, the substantial gap in an otherwise quite even distribution of distances (*cf. Fig. 17*) may be significant, and demonstrate the distinction between normal $Tl-Br$ and secondary $Tl \cdots Br$ bonds. In *Alcock*'s initial treatise on secondary bonding [30], the smallest of the tabulated differences between the lengths of the secondary and normal single bonds is 0.39 Å. Thus, it would be reasonable to assign those $Tl \cdots Br$ distances in the bromothallate(III) salts that are above 3.0 Å as being indicative of secondary bonding.

4.7. *H-bonding Patterns.* The influence of $N-H \cdots Br$ H-bonding on the formation of the $[TlBr_5]^{2-}$ anion has been mentioned above, but it is instructive to summarize the patterns of H-bonding found in all of the bromothallate(III) compounds whose crystal structures have been determined.

- In compounds where the cations have one or more $N-H$ H-bond donors, all available donor H-atoms form H-bonds with anionic Br-atoms.
- In compounds with discrete $[TlBr_5]^{2-}$ anions, all cations are divalent, and none of the cations have H-bond donor atoms.
- In compounds with secondary $Tl \cdots Br$ bonds that result in weak $[TlBr_4] \cdots Br$ association, all cations are divalent, all cations have H-bond donor atoms, and the Br-atom of the secondary $Tl \cdots Br$ bond always accepts multiple H-bonds, but may not be the sole acceptor, with additional H-bonds sometimes involving other Br-atoms, as observed for the piperazinium, 2-(ammoniomethyl)pyridinium, and 1-benzylpiperazinium (**XXI**, **XXIII**, and **IV**, resp.) salts.
- In compounds with discrete $[TlBr_4]^-$ and Br^- ions, all cations have H-bond donor atoms, and all of the H-bonds form exclusively with the discrete Br^- ion. An exception is the pyrazolinium (**V**) salt, where Br^- and $[TlBr_4]^-$ ions act as H-bond acceptors.
- In compounds with mixed discrete anions, such as $[BaseH_2]_3 \cdot [TlBr_4]_3 \cdot [TlBr_6]$ or $[BaseH_2]_4 \cdot [TlBr_4] \cdot [TlBr_6] \cdot 4\,Br$, all cations have H-bond donor atoms, and the $[TlBr_4]^-$ anion never accepts any of the H-bonds.
- The pure $[TlBr_4]^-$ salts are usually the only cases where a $[TlBr_4]^-$ anion acts as an acceptor of $N-H \cdots Br$ H-bonds. Compound **5** is the one exception where $[TlBr_4]^-$ ions accept H-bonds despite the presence of discrete Br^- ions.

- In general, the preference for accepting a $N-H\cdots Br$ H-bond when mixed anions are present appears to follow the pattern $Br^- > [TlBr_6]^{3-} > [TlBr_4]^-$, which reflects the trend in electron density available on each of these species and hence their H-bond acceptor strength.
- The presence of $N-H\cdots Br$ H-bonding interactions decreases the available electron density on the acceptor Br-atom, thus weakening the coordination strength of the Br-atom, and producing a longer $Tl-Br$ bond. This effect is demonstrated dramatically in the salts with varying degrees of $[TlBr_4]\cdots Br$ association, where the H-bonding has influenced the formation of secondary $Tl\cdots Br$ bonds, but also evidently causes slight distortion of the geometry of $[TlBr_6]^{3-}$ anions.

5. Conclusions. – The systematic study of organoammonium bromothallate(III) salts presented here has expanded substantially the number of known bromothallate(III) compounds and broadened our knowledge of the structural diversity that can be exhibited by the anions in these salts. While the structural diversity aspects of the aims have largely been fulfilled, less success can be claimed for the ability to control the type of anionic species generated or for being able to predict when a certain anion might be obtained. The following broad statements can be made.

Discrete $[TlBr_5]^{2-}$ anions can only be obtained if a divalent quaternary organo-ammonium cation is used, or another divalent cation that does not possess H-bond donor atoms. However, the use of such cations does not necessarily guarantee the formation of $[TlBr_5]^{2-}$ anions.

Monovalent cations favor the formation of $[TlBr_4]^-$ species when used in a 1 : 1 ratio with $TlBr_3$, but, again, the use of such cations, even in the correct cation/$TlBr_3$ ratio, does not guarantee the formation of $[TlBr_4]^-$ anions.

In systems expected on stoichiometric and valency grounds to be conducive to the formation of $[TlBr_5]^{2-}$ anions, such as with divalent cations, the presence of H-bonding donor atoms on the cation induces the formation of highly distorted $[TlBr_5]^{2-}$ anions with secondary $Tl\cdots Br$ bonds that may be described as a $[TlBr_4]\cdots Br$ association, or produces structures with discrete $[TlBr_4]^-$ and Br^- ions.

The size, shape, bulkiness, and acidity of the cations have no predictable influence on the nature of the anionic species obtained.

A 1:1 reaction ratio for cation/$TlBr_3$ was maintained in synthesis mixtures throughout this study, and it would be an interesting extension to ascertain if complexes with different stoichiometries and structures could be obtained from the same starting materials if different cation/$TlBr_3$ ratios were employed. Structures with discrete $[TlCl_5]^{2-}$ anions are also quite rare [36][37], because of a tendency to form binuclear or polynuclear anions such as $[Tl_2Cl_{10}]^{4-}$ [38–44], but quaternary ammonium cations have not been used extensively to generate chlorothallate(III) salts, so the question is open as to whether such cations could be employed to obtain discrete $[TlCl_5]^{2-}$ anions or structures similar to or different from those of the bromothallates.

REFERENCES

[1] A. Linden, A. Petridis, B. D. James, *Helv. Chim. Acta* **2003**, *86*, 711.
[2] A. Linden, A. Petridis, B. D. James, *Inorg. Chim. Acta* **2002**, *332*, 61.
[3] A. G. Lee, 'The Chemistry of Thallium', Elsevier, Amsterdam, 1971, Chapt. 3.
[4] A. Linden, K. W. Nugent, A. Petridis, B. D. James, *Inorg. Chim. Acta* **1999**, *285*, 122.
[5] A. Linden, M. A. James, M. B. Millikan, L. M. Kivlighon, A. Petridis, B. D. James, *Inorg. Chim. Acta* **1999**, *284*, 215.
[6] A. Linden, A. Petridis, B. D. James, *Acta Crystallogr., Sect. C* **2002**, *58*, m53.
[7] G. Brauer, 'Handbook of Preparative Inorganic Chemistry', Vol. 1, 2nd edn., Academic Press, New York, 1963, p. 869 and 874.
[8] S. Oae, B. Hovarth, C. Zalut, R. Harris, *J. Org. Chem.* **1959**, *24*, 1348.
[9] K. Nakamoto, 'Infrared and Raman Spectra of Inorganic and Coordination Compounds', 4th edn., John Wiley & Sons, New York, 1986.
[10] R. Hooft, KappaCCD Collect Software, *Nonius BV*, Delft, The Netherlands, 1999.
[11] Z. Otwinowski, W. Minor, in 'Methods in Enzymology', Vol. 276, 'Macromolecular Crystallography, Part A', Eds. C. W. Carter Jr., R. M. Sweet, Academic Press, New York, 1997, pp. 307–326.
[12] R. H. Blessing, *Acta Crystallogr., Sect. A* **1995**, *51*, 33.
[13] P. Coppens, L. Leiserowitz, D. Rabinovich, *Acta Crystallogr.* **1965**, *18*, 1035.
[14] A. Altomare, G. Cascarano, C. Giacovazzo, A. Guagliardi, M. C. Burla, G. Polidori, M. Camalli, SIR92, *J. Appl. Crystallogr.* **1994**, *27*, 435.
[15] H. D. Flack, G. Bernardinelli, *Acta Crystallogr., Sect. A* **1999**, *55*, 908.
[16] H. D. Flack, G. Bernardinelli, *J. Appl. Crystallogr.* **2000**, *33*, 1143.
[17] E. N. Maslen, A. G. Fox, M. A. O'Keefe, 'International Tables for Crystallography', Ed. A. J. C. Wilson, Kluwer Academic Publishers, Dordrecht, 1992, Vol. C, Table 6.1.1.1, pp. 477–486.
[18] R. F. Stewart, E. R. Davidson, W. T. Simpson, *J. Chem. Phys.* **1965**, *42*, 3175.
[19] J. A. Ibers, W. C. Hamilton, *Acta Crystallogr.* **1964**, *17*, 781.
[20] D. C. Creagh, W. J. McAuley, 'International Tables for Crystallography', Ed. A. J. C. Wilson, Kluwer Academic Publishers, Dordrecht, 1992, Vol. C, Table 4.2.6.8, pp. 219–222.
[21] D. C. Creagh, J. H. Hubbell, 'International Tables for Crystallography', Ed. A. J. C. Wilson, Kluwer Academic Publishers, Dordrecht, 1992, Vol. C, Table 4.2.4.3, pp. 200–206.
[22] G. M. Sheldrick, SHELXL97, Program for the Refinement of Crystal Structures, University of Göttingen, Göttingen, 1997.
[23] C. K. Johnson, ORTEPII, Report ORNL-5138, Oak Ridge National Laboratory, Oak Ridge, Tennessee, USA, 1976.
[24] A. L. Spek, PLATON, Program for the Analysis of Molecular Geometry, University of Utrecht, The Netherlands, 2004.
[25] F. Basolo, *Coord. Chem. Rev.* **1968**, *3*, 213.
[26] T. G. Spiro, *Inorg. Chem.* **1967**, *6*, 569.
[27] J. Blixt, J. Glaser, J. Mink, I. Persson, P. Persson, M. Sandström, *J. Am. Chem. Soc.* **1995**, *117*, 5089.
[28] J. Glaser, G. Johansson, *Acta Chem. Scand., Ser. A* **1982**, *36*, 125.
[29] CAChe MOPAC Guide, Version 3.9 for the CAChe Work System, Oxford Molecular Group, Beaverton, Oregon, USA, 1996, p. 16.
[30] N. W. Alcock, *Adv. Inorg. Chem. Radiochem.* **1972**, *15*, 1.
[31] N. W. Alcock, 'Bonding and Structure', Horwood, Chichester, 1990.
[32] J. Bernstein, R. E. Davis, L. Shimoni, N.-L. Chang, *Angew. Chem., Int. Ed.* **1995**, *34*, 1555.
[33] J. Dijkink, K. Eriksen, K. Goubitz, M. N. A. van Zanden, H. Hiemstra, *Tetrahedron: Asymmetry* **1996**, *7*, 515.
[34] W. M. Reiff, S. M. Smith, B. D. James, J. Liesegang, B. W. Skelton, A. H. White, Abstracts of the 212th American Chemical Society National Meeting, Orlando, USA, 1996, Abstract INOR 105.
[35] K. F. Bowes, G. Ferguson, A. J. Lough, C. Glidewell, *Acta Crystallogr., Sect. B* **2003**, *59*, 100.
[36] M. A. James, M. B. Millikan, B. D. James, *Main Group Met. Chem.* **1991**, *14*, 1.
[37] M. Abdi, F. Zouari, A. Ben Salah, *J. Chem. Crystallogr.* **2004**, *34*, 673.

[38] G. Thiele, H. W. Rotter, M. Faller, *Z. Anorg. Allg. Chem.* **1984**, *508*, 129.
[39] M. A. James, J. A. C. Clyburne, A. Linden, B. D. James, J. Liesegang, V. Zuzich, *Can. J. Chem.* **1996**, *74*, 1490.
[40] G. Thiele, R. Richter, *Z. Kristallogr.* **1993**, *205*, 131.
[41] M. Abdi, F. Zouari, S. Chaabouni, A. Ben Salah, *J. Chem. Crystallogr.* **2003**, *33*, 839.
[42] M. Abdi, F. Zouari, A. Ben Salah, *Solid State Sci.* **2004**, *6*, 739.
[43] N. Chaari, S. Chaabouni, N. Chniba-Boudjada, P. Bordet, A. Ben Salah, *Anal. Sci.: X-Ray Struct. Anal. Online* **2007**, *23*, x5.
[44] N. Chaari, S. Chaabouni, A. Hadrich, A. Ben Salah, *Ann. Chim. (Fr.)* **2007**, *32*, 531.
[45] R. Al-Far, B. F. Ali, *Acta Crystallogr., Sect. E* **2007**, *63*, m2242.
[46] M. Abdi, F. Zouari, N. Chniba-Boudjada, P. Bordet, A. Ben Salah, *Acta Crystallogr., Sect. E* **2005**, *61*, m240.